IEEE Access
Multidisciplinary | Rapid Review | Open Access Journal

Received January 20, 2018, accepted February 27, 2018, date of publication March 7, 2018, date of current version April 4, 2018.

Digital Object Identifier 10.1109/ACCESS.2018.2813081

Impact of Residual Hardware Impairments on Non-Orthogonal Multiple Access Based Amplify-and-Forward Relaying Networks

FAN DING[1], (Member, IEEE), HUI WANG[2], SHENGLI ZHANG[2], (Member, IEEE), AND MINGJUN DAI[2], (Member, IEEE)

[1]School of Physics and Electromechanical Engineering, Shaoguan University, Shaoguan 512000, China
[2]Department of Communication Engineering, Shenzhen University, Shenzhen 518060, China

Corresponding author: Fan Ding (dingfan82@163.com)

The work was supported in part by research grants from the Key Project of Shaoguan University of China under Grant SZ2017KJ08, in part by the Science and Technology Program of Shaoguan City, China, under Grant SK20157202, in part by the Chinese NSF Project under Grant 61771315, in part by the Shenzhen NSF Project under Grant JCYJ20160226192223251, in part by the Key Project of Department of Education of Guangdong Province under Grant 2015KTSCX121, and in part by the Natural Science Foundation of Shenzhen University under Grant 00002501.

ABSTRACT We quantify the impact of residual hardware impairments (RHI) on a non-orthogonal multiple access (NOMA)-based relaying network, where a source communications simultaneously with multiple users via an amplify-and-forward relay. Specifically, exact and asymptotic expressions for the outage probability are first derived in closed-form over Nakagami-*m* fading channels, accounting for RHI at the source, relay, and all users. Our results show that the outage performance loss induced by RHI is small in the low signal-to-noise ratio (SNR) regime or/and at low target rates, however it is significant at high SNRs or/and target rates. Furthermore, we present new tight analytical approximated and asymptotic expressions for the system ergodic sum rate (ESR). For comparison, we also discuss the ESR of the conventional hardware-impaired relaying system employing orthogonal multiple access (OMA) transmission and obtain the asymptotic high-SNR expression of the ESR. The provided numerical results demonstrate that in the absence of RHI, the ESR in either the NOMA or the OMA system increases monotonically with the increase of SNR, whereas an unavoidable ESR ceiling is introduced in the hardware-impaired scenario for both systems. Notably, since the ESR ceiling value is only depended on the RHI levels, the NOMA-based and OMA-based systems achieve the same ESR performance in high SNRs.

INDEX TERMS Non-orthogonal multiple access, residual hardware impairments, outage probability, ergodic sum rate.

I. INTRODUCTION

Recently, non-orthogonal multiple access (NOMA) has been regarded as one promising technology in future fifth-generation (5G) wireless networks to improve spectral efficiency [1]. Compared with orthogonal multiple access (OMA), NOMA can provide improved spectral efficiency and user fairness by allowing multiple users to be served in the same time, frequency or code domain. In particular, multiple users' messages are superposed at the transmitter and successive interference cancellation (SIC) is adopted at the receivers to separate the mixture signals in the power domain [2]. In [3], NOMA transmission in a typical single-hop cellular system was considered, in which the system performance in terms of outage probability (OP) and ergodic sum rate (ESR) was investigated. The subsequent work in [4] studied the power allocation with max-min fairness criterion. Recently, NOMA has been applied to large-scale underlay cognitive radio (CR) networks [5].

A. COOPERATIVE RELAYING WITH NOMA

More recent works have considered the integration of cooperative relaying transmission with NOMA systems, where users or/and dedicated relays cooperative to further improve the spectral efficiency and transmission reliability of NOMA systems [6]–[16]. Specifically, in [6], a cooperative NOMA (C-NOMA) scheme was first proposed for a NOMA-based cellular network with multiple users, where users with strong channel conditions acted as relays to assist

the users with weak channel conditions. In [7], simultaneous wireless information and power transfer (SWIPT) technique was used in C-NOMA systems, in which near NOMA users that are close to the source act as energy harvesting relays to help far NOMA user. Additionally, the concept of C-NOMA was considered in overlay CR networks, where a secondary transmitter [8] or a secondary receiver [9] serves as a relay and helps transmit the primary messages, so as to access same the frequency band allocated to the primary network. On the other hand, a dedicated relay can be employed to improve the performance of NOMA systems [10]–[16]. In [10] and [11], NOMA was applied to the classical three-nodes cooperative relaying system (CRS) with a dedicated half-duplex relay, where the source transmits two symbols with different power levels using superposition coding so that the destination can acquire two data symbols during two times slots. In [12] and [13], two-user NOMA systems were considered, where the authors proposed to employ a dedicated half-duplex relay [12] or a dedicated full-duplex relay [13] to improve the performance of the user with poor channel condition. Furthermore, for multi-user NOMA systems without direct link transmissions as in [14], a variable gain relay was introduced to facilitate the transmission between the source and NOMA users. Under Nakagami-*m* fading channels, exact and asymptotic high signal-to-noise ratio (SNR) expressions for the OP and ESR was presented to show the superiority of NOMA over OMA. Recently, the work of [14] was extended to NOMA-based relaying networks with a fixed gain relay and direct link transmissions [15]. Very recently, a NOMA-based relaying network with a SWIPT-based decode-and-forward (DF) relay was considered in [16].

Common to the aforementioned research contributions is the strong assumption of the ideal transmitter-receiver hardware structures and this assumption is idealistic for practical applications. In practice, the hardware gear of wireless transceivers may be subject to impairments, such I/Q imbalance (IQI), high power amplifier (HPA) non-linearities and oscillator phase noises [17]. The related works on hardware impairments are detailed in the next subsection.

B. LITERATURE REVIEW ON HARDWARE IMPAIRMENTS

The impact of *individual* hardware impairments on different types of wireless systems has been well investigated [18]–[22]. As a general conclusion, the individual [18]–[20], [22] or the combined [21] hardware impairments have a deleterious impact on the achievable performance.

Generally speaking, the performance degradation caused by the above single type of hardware impairments can be typically mitigated by using certain calibration techniques at the transmitter or/and compensation algorithms at the receiver [17]. However, these approaches are not able to completely remove hardware impairments, and hence there always remains a certain amount of unaccounted distortion caused due to residual hardware impairments (RHI), which are added to the transmitted/received signal [17]. These RHI stem from inadequate compensation schemes resulting from the imperfect parameter estimation and/or time variation of the hardware characteristics, the randomness of noises, and etc [17], [23], [24]. Recently, the performance analysis of various cooperative relaying systems suffering from RHI has attracted considerable attentions [25]–[30]. Specifically, exact and asymptotic expressions of OP and the ergodic capacity of AF and DF relaying systems were derived in [25], where RHI in all nodes are considered. In [26], the authors analyzed the impact of RHI at the relay on the OP and symbol error rate in a two-way relaying configuration. Similarly, the OP of cognitive AF multirelay networks was derived in [27] considering only RHI at the relay. Recently, the joint impact of RHI and co-channel interference (CCI) or channel estimation error on OP or/and average capacity was investigated in [28] and [29], respectively. Very recently, the effects of RHI on the OP of a hybrid satellite-terrestrial relay network was analyzed in [30].

C. MOTIVATION AND CONTRIBUTIONS

As described above, residual transceiver hardware impairments may significantly degrade the performance of the conventional OMA-based relaying networks. Nevertheless, there is no previous work focusing on the effect of RHI on the newly NOMA-based two-hop relaying configuration or even the single-hop NOMA systems, to the best of the authors knowledge. his motives the work of this paper. Specifically, we analyze the performance of a NOMA-based relaying network as considered in [14], whereas we take the aggregate residual hardware impairments at all nodes into consideration. We attempt to present a framework of analyzing the effect of RHI on a NOMA-based relaying network. The analysis utilizes the generalized residual impairment model of [17], which can provide a macroscopic look at the aggregate impact of diverse residual hardware impairments in a NOMA-based relaying configuration. The key contributions are as follows:

- Under Nakagami-*m* fading channels, we first derive exact closed-form expressions for the users' outage probabilities, which provide accurate characterizations of the impact of RHI on user's OP for any arbitrary SNR value.
- To gain more engineering insights, we then present asymptotic high-SNR expressions of users' outage probabilities. We find that, if the *critical condition* that users' target rates and power coefficients are properly chosen, the presence of RHI does not affect the user's obtained diversity order, rather it decreases the array gain, thus increasing the OP. In particular, the OP of the hardware-impaired NOMA system turns out to be more sensitive to the choices of the target rates and power coefficients, compared to the ideal NOMA system. It is worth mentioning that unified exact closed-form and asymptotic OP expressions of each user in NOMA-based AF relaying network with and without RHI are derived in this paper. Therefore, our work includes the

work in [14] as a special case where ideal hardware is assumed.

- Furthermore, for the NOMA-based AF relaying network with/without RHI, a unified accurate approximation of the individual ergodic rate (IER) of each user is derived in closed-form, from which a tight analytical formula for the system ESR is obtained in a straightforward manner. It is worth noting that exact expression for the IER or ESR of NOMA-based AF relaying systems is difficult to obtain, as stated in [14]. In this context, the lower and upper bounds for the user with the best channel gain (best user) are derived in [14], while both of them are generally loose over the entire SNR range. However, as for the non-best users, only the high-SNR asymptotic expressions are presented. In this paper, by using the method of second order Taylor series approximation as proposed in [31], we provide unified accurate approximations for the IER and system ESR, which generally enable an accurate characterization of the capacity behavior of NOMA-based AF networks for arbitrary SNR values and other different system configurations.
- Finally, simple asymptotic expressions for the IER and ESR are derived. Interestingly, the asymptotic results reveal that the presence RHI results in a ceiling effect on the system ESR, which depends only on the hardware impairment levels, whereas the asymptotic ESR of ideal-hardware system scales as $\frac{1}{2}\log_2\rho$, where ρ denotes the system SNR. In addition, a comparison in ESR performance between the NOMA-based system and the typical orthogonal multiple access (i.e., time division multiple access) based system is provided. The present analytical and numerical results confirm that the ESR of NOMA-based relaying system without RHI is superior to that of the OMA-based relaying system at moderate-to-high SNRs. However, the high-SNR asymptotic ESR of both systems are exactly the same, due to the presence of RHI.

D. ORGANIZATION AND NOTATIONS

The rest of this paper is organized as follows. In Section II, the system model, for NOMA-based AF relaying networks with RHI, are presented. In Section III, we derived exact and asymptotic expressions of outage probability for users. In Section IV, tight analytical and asymptotic expressions of the ergodic rate for each user are presented, form which the expressions of the system ergodic sum rate are obtained. Section V presents simulation results to verify our theoretical analysis. Finally, Section VI concludes the paper.

Notations: Throughout this paper, $f_X(\cdot)$ and $F_X(\cdot)$ denote the probability density function (PDF) and the cumulative distribution function (CDF) of a positive random variable X, respectively; $\mathbb{E}[\cdot]$ denotes the expectation and $\Pr(\mathcal{A})$ is the probability of an event $\mathcal{A}$. The operator $\triangleq$ denotes a definition. $\mathcal{CN}(a,\sigma^2)$ denotes the complex Gaussian distribution with mean a and variance σ^2. $\Gamma(\cdot)$ is the Gamma function [35], and $K_v(\cdot)$ denotes the vth-order modified Bessel function of the second kind [35].

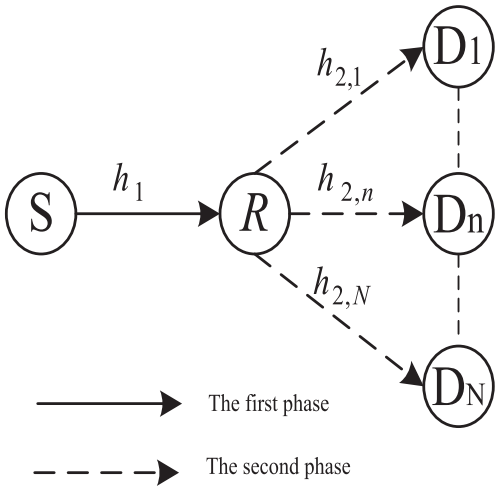

FIGURE 1. NOMA-based AF relaying system.

II. SYSTEM MODEL WITH RESIDUAL HARDWARE IMPAIRMENTS

We consider a downlink NOMA-based relay network as shown in Fig. 1, where one source S communicates with N users $\{D_n\}_{n=1}^N$ simultaneously via the help of an AF relay R. All nodes are equipped with single antenna and operate in a time-division half-duplex mode. No direct links exist between the source and the destinations, due to the long distance or significant obstacle.

The channel coefficients of the $S \rightarrow R$ link and the $R \rightarrow D_n$ link are denoted by h_1 and $h_{2,n}$, respectively. Then, in a Nakagami-m fading environment, the channel gains $|h_1|^2$ and $|h_{2,n}|^2$ follow the Gamma distribution with different fading severity parameters m_i and different average fading powers Ω_i, $i = \{1, 2\}$, respectively, where $\mathbb{E}[|h_1|^2] = \Omega_1$, and $\mathbb{E}[|h_{2,n}|^2] = \Omega_{2,n}$ with $\mathbb{E}[\cdot]$ is the expectation operator. Moreover, we consider a homogeneous network topology for mathematical tractability, where all users are located in close proximity to each other. In such a homogeneous environment, all channels between the relay and users experience independent and identically distributed (i.i.d) Nakagami-m fading, i.e., $\Omega_2 \triangleq \Omega_{2,n}$ and $m_2 \triangleq m_{2,n}$. Note that this assumption is widely adopted in NOMA-based systems to facilitate the analysis (please see [7], [8], [14] for more details). Besides, the AWGN n_a at each receiver a ($a \in \{R, D_n\}$) is modeled as a complex Gaussian variable with zero mean and variance σ^2, i.e., $n_a \sim \mathcal{CN}(0, \sigma^2)$. For simplicity, we assume $\sigma^2 = 1$ hereafter.

A. NOMA TRANSMISSION

In NOMA-based AF networks, the communication is conducted in two phases. In phase 1, the source S sends $\sum_{n=1}^N \sqrt{\alpha_n P_s} x_n$ to the relay R according to NOMA principle, where P_s is the transmitted power of S, x_n is the message for

n-th user (i.e., D_n), and α_n is the power allocation coefficient with $\sum_{n=1}^{N}\alpha_n = 1$. In the presence of RHI, the received signal at R is given by

$$y_R = h_1\left(\sum_{n=1}^{N}\sqrt{\alpha_i P_s}x_n + \eta_{sr}\right) + n_R, \tag{1}$$

where the independent distortion noise $\eta_{sr} \sim \mathcal{CN}(0, \kappa_{SR}^2 P_s)$ denotes the RHI at both the transmitter (S) and the receiver (R), and $\kappa_{SR} \triangleq \sqrt{\kappa_{S,t}^2 + \kappa_{R,r}^2}$ describes the aggregate level of RHI of the $S \to R$ link, where $\kappa_{S,t}$ and $\kappa_{R,r}$ characterize the hardware impairments levels in S and R, respectively. Note that these parameters, i.e., $\kappa_{S,t}, \kappa_{R,r} \geq 0$, are measured as error vector magnitudes (EVMs). The typical values of hardware impairment lie in the range of [0.08, 0.175], which resemble the EVMs of 3GPP Long Term Evolution (LTE) requirements as mentioned in [32, Sec.14.3.4].

In phase 2, R amplifies the received signal y_R with a gain factor $\mathcal{G}$, and then broadcasts it to all users with power P_r. For variable gain relaying, the amplifying gain is given by [25]

$$\mathcal{G} = \sqrt{\frac{P_r}{(1+\kappa_{SR}^2)P_s|h_1|^2 + 1}}. \tag{2}$$

Then, considering the RHI at the relay and D_n, the received signal at D_n is $y_{D_n} = h_{2n}(\mathcal{G}y_R + \eta_{2,n}) + n_{D_n}$, and it can be further expressed by

$$\begin{aligned} y_{D_n} &= h_{2,n}\mathcal{G}\left[h_1\left(\sum_{n=1}^{N}\sqrt{\alpha_n P_s}x_n + \eta_{sr}\right) + n_R\right] \\ &\quad + h_{2,n}\eta_{2,n} + n_{D_n} \\ &= \mathcal{G}h_1h_{2,n}\sqrt{P_s}\Bigg(\underbrace{\sum_{k=1}^{n-1}\sqrt{\alpha_k}x_k}_{\text{SIC}} + \underbrace{\sqrt{\alpha_n}x_n}_{\text{signal}} \\ &\quad + \underbrace{\sum_{j=n+1}^{N}\sqrt{\alpha_j}x_j}_{\text{IUI}}\Bigg) + \underbrace{\mathcal{G}h_1h_{2,n}\eta_1 + h_{2,n}\eta_{2,n}}_{\text{THI distrotion noises}} \\ &\quad + \underbrace{\mathcal{G}h_{2,n}n_R + n_{D_n}}_{\text{noises}}, \end{aligned} \tag{3}$$

where $\eta_{2,n} \sim \mathcal{CN}(0, \kappa_{RD_n}^2 P_r)$ is the RHI induced aggregate distortion noise of the $R \to D_n$ link. In addition, $\kappa_{RD_n} = \sqrt{\kappa_{R,t}^2 + \kappa_{D_n,r}^2}$ is the aggregate level of RHI of the $R \to D_n$ link, where $\kappa_{R,t}$ and $\kappa_{D_n,r}$ denote the levels of hardware impairments in R and D_n, respectively. Similar to [27], [28] and [30], we assume that all users have the same structure to facilitate the analysis. As such, the impairment levels of users are the same, i.e., $\kappa_{D,r}^2 = \kappa_{D_n,r}^2$. Accordingly, we define $\kappa_{RD} \triangleq \kappa_{RD_n} = \sqrt{\kappa_{R,t}^2 + \kappa_{D,r}^2}$. It is worthwhile noting that in case of different levels of hardware impairment, our results can be applied to derive the upper-bound and/or lower-bound of the outage probability and ergodic rate of each user.

B. SIC DECODING AT USERS

Without loss of generality, we assume all users are ordered based on their channel qualities: $|h_{2,1}|^2 \leq \cdots \leq |h_{2,N}|^2$. In NOMA systems, users with poorer channel qualities are allocated more transmission powers [2]. This implies that users' power allocation factors are ordered as $\alpha_1 \geq \cdots \geq \alpha_N$. According to the NOMA principle, SIC is carried out at D_n to separate the mixture signals in the power domain [3]. Specifically, D_n will first decode signal of the weaker user[1] D_k ($k < n$) (the 'SIC' term in (3)) and removes it from its observation in a successive manner [3]. While the stronger user D_j's signal (the 'inter-user interference' (IUI) term in (3)), $j > n$, will be treated as noise at D_n. Therefore, from (3), the signal-to-interference-plus-distortion-and-noise ratio (SIDNR) of D_k's ($k \leq n$) message decoded by D_n is given by

$$\gamma_{k\to n} = \frac{\alpha_k \mathcal{G}^2 P_s|h_1|^2|h_{2n}|^2}{\left[\mathcal{G}^2|h_{2n}|^2\left(\left(\sum_{j=k+1}^{N}\alpha_j + \kappa_{SR}^2\right)P_s|h_1|^2 + 1\right) + \kappa_{RD}^2|h_{2n}|^2 + 1\right]}. \tag{4}$$

Let $d_0 = \kappa_{SR}^2 + \kappa_{RD}^2 + \kappa_{SR}^2\kappa_{RD}^2$, $d_1 = 1 + \kappa_{SR}^2$, and $d_2 = 1 + \kappa_{RD}^2$. Invoking $\mathcal{G}^2$ into (4), and after some algebraic steps, the SIDNR at D_k is given by

$$\begin{aligned} \gamma_{k\to n} &= \frac{\alpha_k X Y_n}{(\sum_{j=k+1}^{N}\alpha_j + d_0)XY_n + d_1X + d_2Y_n + 1} \\ &= \frac{\alpha_k Z_n}{(\sum_{j=k+1}^{N}\alpha_j + d_0)Z_n + 1}, \end{aligned} \tag{5}$$

where $X \triangleq P_s|h_1|^2$, $Y_n \triangleq P_r|h_{2n}|^2$, and $Z_n \triangleq \frac{XY_n}{d_1X + d_2Y_n + 1}$ with $1 \leq n \leq N$. For the case $n = k$ in (4) and (5), it denotes that D_n decodes its own signal and the SIDNR at D_n is

$$\gamma_n \triangleq \gamma_{n\to n} = \frac{\alpha_n Z_n}{(\sum_{j=n+1}^{N}\alpha_j + d_0)Z_n + 1}, \tag{6}$$

Further, the signal-to-distortion-plus-noise ratio (SDNR) for the strongest user D_N to decode its own message, after all the poorer users' messages are successfully decoded and removed from its received signal, can be expressed by

$$\begin{aligned} \gamma_N \triangleq \gamma_{N\to N} &= \frac{\alpha_N XY_N}{d_0XY_N + d_1X + d_2Y_N + 1} \\ &= \frac{\alpha_N Z_N}{d_0Z_N + 1}. \end{aligned} \tag{7}$$

By invoking $\kappa_{sr} = \kappa_{rd} = 0$ (or equally $d_0 = 0$ and $d_1 = d_2 = 1$) into (5), (6), and (7), they reduce to the ideal-case forms [14]. For instance, in the ideal scenario, (5) is reduced to $\gamma_{k\to n}^{id} = \frac{\alpha_k XY_n}{(\sum_{j=k+1}^{N}\alpha_j)XY_n + X + Y_n + 1}$. We see that the

[1] By saying "weaker user" or "pooer user", it specifies the user that has weaker/poorer *channel gain*, as compared to the user that is under discussion. Similarly, the "stronger user" implies that it has better *channel gain* than the user being discussed.

expressions of $\gamma_{k\to n}$ and $\gamma_{k\to n}^{id}$ have similar forms, except that the coefficients of the variables in their denominators, i.e., XY_n, X, and Y_n, are different. Thus, the presence of RHI does not affect the diversity order in terms of the user's outage probability in general (see Corollary 1 and footnote 5 in Section III).

Besides, from (5), the corresponding data rate achieved at D_n to detect D_k's message is

$$R_{k\to n} = \frac{1}{2}\log_2\left(1+\gamma_{k\to n}\right), \quad 1 < k < n \le N. \tag{8}$$

Similarly, according to (6) and (7), the achievable data rate for D_n to detect its own message is

$$R_n = \frac{1}{2}\log_2\left(1+\gamma_n\right), \quad 1 \le n \le N. \tag{9}$$

III. OUTAGE PROBABILITY PERFORMANCE ANALYSIS

In this section, we consider the case that each user has a preset target rate which is determined by its quality of service (QoS) requirement [3]. In this situation, the outage probability is an ideal metric for performance evaluation as it measures the ability of NOMA to meet the users' predefined QoS requirement [3], [14], especially for a delay-sensitive networks.[2] Specifically, both the exact and asymptotic expressions of each user's individual OP are derived, from which the achievable diversity order is obtained.

A. OUTAGE EVENTS AND UPPER BOUND ON THE TARGET RATE

The outage events at D_n can be defined as follows. We first define $E_{n,k} \triangleq \{R_{k\to n} \ge \widehat{R}_k\}$ as the *non-outage* event that D_n cannot detect D_k's message, $1 \le k \le n$. Here, $\widehat{R}_k$ denote the target rate of D_k. In NOMA, an outage occurs at D_n when it can detect any of k-th user's message, where $k \le n$ due to the SIC [5]. Therefore, the OP at D_n is given by

$$P_{out}^{n} = 1 - \Pr\left(E_{n,1} \cap \cdots \cap E_{n,n}\right). \tag{10}$$

From (5) and (8), the event $E_{n,k}$ can be expressed as

$$\begin{aligned} E_{n,k} &= \left\{ \left[\frac{\alpha_k}{2^{2\widehat{R}_k}-1} - \left(\sum_{j=k+1}^{N}\alpha_j + d_0\right)\right] XY_n \right. \\ &\quad \left. > d_1 X + d_2 Y_n + 1 \right\} \\ &\overset{(a)}{=} \left\{ Z_n > \left(\frac{\alpha_k}{2^{2\widehat{R}_k}-1} - \left(\sum_{j=k+1}^{N}\alpha_j + d_0\right)\right)^{-1} \right\}, \end{aligned} \tag{11}$$

where step (a) is obtained based on the following critical condition $\frac{\alpha_k}{2^{2\widehat{R}_k}-1} - \left(\sum_{j=k+1}^{N}\alpha_j + d_0\right) > 0$. That is,

$$\widehat{R}_k < \widehat{R}_k^{up} \triangleq \frac{1}{2}\left(1 + \frac{\alpha_k}{\sum_{j=k+1}^{N}\alpha_j + d_0}\right), \quad k \le n. \tag{12}$$

$\widehat{R}_k^{up}$ in (12) is an *upper bound* on the target rate $\widehat{R}_k$, above which decoding D_k's message is impossible at D_n. This has an intuitive explanation since the SIDNR $\gamma_{k\to n}$ in (5) is upper bounded as $\gamma_{k\to n} \le \gamma_k^{up} \triangleq \frac{\alpha_k}{\sum_{j=k+1}^{N}\alpha_j + d_0}$. The existence of $\widehat{R}_k^{up}$ is attributed to the combined effect of RHI and IUIs from the stronger users (i.e., $D_j, j > k$), since both IUIs and RHI induced noises show up interference terms at D_n that are proportional to the transmit power and go through the same channels as the intend signal x_n (see (3)). Therefore, as shown in (12), the value of the upper bound is characterized by the power allocation (PA) coefficients and RHI levels.

By setting $d_0 = 0$ in (12), the upper bound of $\widehat{R}_k$ in NOMA without RHI is obtained as

$$\widehat{R}_{k,id} < \widehat{R}_{k,id}^{up} \triangleq \frac{1}{2}\left(1 + \frac{\alpha_k}{\sum_{j=k+1}^{N}\alpha_j}\right). \tag{13}$$

Equation (13) implies that in the ideal NOMA system, there still exists an upper bound $\widehat{R}_{k,id}^{up}$ on the target rate $\widehat{R}_k$. Note that, unlike NOMA with RHI, the existence of $\widehat{R}_{k,id}^{up}$ in the ideal case results from the IUIs only and thus it is dependent only on the PA coefficients.

Similarly, we define $E_{N,N} \triangleq \{R_N \ge \widehat{R}_N\}$ as the *non-outage* event that D_N can detect its own message. From (7) and (9), the event $E_{N,N}$ can be expressed as

$$E_{N,N} = \left\{ Z_N \ge \left(\frac{\alpha_N}{2^{2\widehat{R}_N}-1} - d_0 \right)^{-1} \right\}. \tag{14}$$

which is obtained based on the following condition:

$$\widehat{R}_N < \widehat{R}_N^{up} \triangleq \frac{1}{2}\left(1 + \frac{\alpha_N}{d_0}\right). \tag{15}$$

The result in (15) implies that even if all the weaker users' messages can be decoded at the best user D_N, i.e., D_N is free from IUIs, there still exists an upper bound $\widehat{R}_N^{up}$ due to the presence of RHI. However, there does not exist such an upper bound on the target rate of D_N in the ideal NOMA system.

Remark 1: From (12), we see that the upper bound $\widehat{R}_k^{up}$ is independent of the transmit power, and hence it cannot be crossed by simply increasing the transmit power. More importantly, $\widehat{R}_k^{up}$ is also irrespective of the channel gains. From this observation, we conclude that when $\widehat{R}_k \ge \widehat{R}_k^{up}$, not only D_k cannot detect its own signal x_k, but also all stronger users (i.e., $D_{k+1},\ldots, D_N$) cannot detect x_k before detecting their desired signals. Intuitively, substituting (5) into (8) and using the fact $|h_{2,1}|^2 \le \cdots \le |h_{2,N}|^2$, we have $R_{k\to k} \le R_{k\to k+1} \le \ldots \le R_{k\to N} < \widehat{R}_k^{up}$. In other words, as long as $\widehat{R}_k \ge \widehat{R}_k^{up}$, outage will occur at D_n where $k \le n \le N$. For example, if $\widehat{R}_2 \ge \widehat{R}_2^{up}$, the users $D_2, D_3, \ldots, D_N$ will be in full outage. In particular, if $\widehat{R}_1 \ge \widehat{R}_1^{up}$, all the users (including

[2] In wireless communication systems, the BER is another important performance metric. However, as sated in [16], it is difficult to obtain the exact BER of NOMA-based system in closed-form as they depends on the specific channel coding or modulation schemes. Moreover, the error propagation effect due to imperfect SIC makes the analysis of exact BER in NOMA very challenging, and thus no prominent research that provides a rigorous mathematical understanding of the effect of imperfect SIC on NOMA schemes [2]. In this context, the benefit of using OP in NOMA is also manifested in making the mathematical analysis simple and tractable. In particular, the fundamental limits of a wireless communication system using specific channel coding or modulation can be evaluated by OP, since the probability of detection error can tightly bounded by the OP when optimal coding with an infinite length is used.

the user D_1) are always in outage. Similar conclusions can be drawn in the ideal-hardware NOMA system.

B. EXACT OP

From the above analysis, the outage probability of D_n in (10) can be rewritten as

$$P_{out}^{n} = \begin{cases} 1 - \Pr\left(E_{n,1} \cap \cdots \cap E_{n,n}\right), & \widehat{R}_k < \widehat{R}_k^{up} \\ 1, & \widehat{R}_k \geq \widehat{R}_k^{up}, \end{cases} \quad (16)$$

where $1 \leq k \leq n \leq N$.

Define $\varepsilon_n = \left(\frac{\alpha_n}{2^{2\widehat{R}_n}-1} - \left(\sum_{j=n+1}^{N} \alpha_j + d_0\right)\right)^{-1}$ with $1 \leq n \leq N-1$, $\varepsilon_N = \left(\frac{\alpha_N}{2^{2\widehat{R}_N}-1} - d_0\right)^{-1}$, and $\varepsilon_n^* = \max\{\varepsilon_1, \cdots, \varepsilon_n\}$ for $1 \leq n \leq N$. Then, invoking (11) or/and (14) into (16), we can express (16) as follows

$$P_{out}^{n} = \begin{cases} 1 - \Pr\left(Z_n > \varepsilon_n^*\right) = F_{Z_n}(\varepsilon_n^*), & \widehat{R}_k < \widehat{R}_k^{up} \\ 1, & \widehat{R}_k \geq \widehat{R}_k^{up}, \end{cases} \quad (17)$$

where $F_{Z_n}(x)$ denotes the cumulative distribution function (CDF) of Z_n. Without loss of generality, we assume that $P_s = P_r = P$ [14], and refer to $\rho \triangleq P/\sigma^2$ as the average system SNR. Accordingly, we have $X = \rho|h_1|^2$ and $Y_n = \rho|h_{2n}|^2$.

The following theorem provides new and tractable closed-form OP expression of D_n in the presence of RHI.

Theorem 1: For Nakagami-m fading channels with integer fading parameters, the OP of D_n in NOMA-based AF networks with RHI is derived as

$$\begin{aligned} P_{out}^{n} = 1 - \frac{Q_n}{\Gamma(m_2)} & \sum_{i_1=0}^{m_1-1} \sum_{j_1=0}^{i_1} \sum_{i_2=0}^{N-n} \sum_{j_2=0}^{n+i_2-1} \widetilde{\sum_{j_2,n_\ell}} \sum_{k_2=0}^{m_2+\Phi_{n_\ell}-1} \\ & \times \frac{\binom{i_1}{j_1}}{i_1!} \Lambda(i_2, j_2, n_\ell, k_2) e^{-\left(\frac{m_1 d_2}{\Omega_1} + \frac{(j_2+1)m_2 d_1}{\Omega_2}\right)\frac{\varepsilon_n^*}{\rho}} \\ & \times \left(\frac{m_1 d_2 \varepsilon_n^*}{\rho \Omega_1}\right)^{i_1} \left(\frac{m_2 d_1 \varepsilon_n^*}{\rho \Omega_2}\right)^{m_2+\Phi_{n_\ell}} \left(d_1 \varepsilon_n^* + \frac{1}{d_2}\right)^{j_1} \\ & \times \left(\frac{m_1 \Omega_2 \varepsilon_n^* (d_1 d_2 \varepsilon_n^* + 1)}{(j_2+1) m_2 \Omega_1}\right)^{\frac{k_2 - j_1 + 1}{2}} (d_1 \varepsilon_n^*)^{-k_2-1} \\ & \times 2K_{k_2-j_1+1}\left(\frac{2}{\rho}\sqrt{\frac{(j_2+1)m_1 m_2 d_1 d_2 \varepsilon_n^*}{\Omega_1 \Omega_2 (\varepsilon_n^* + \frac{1}{d_1 d_2})^{-1}}}\right), \end{aligned} \quad (18)$$

for $\widehat{R}_k < \widehat{R}_k^{up}$ and $P_{out}^{n} = 1$ for $\widehat{R}_k \geq \widehat{R}_k^{up}$, where $1 \leq k \leq n \leq N$. Here, $Q_n = \frac{N!}{(N-n)!(n-1)!}$, $\widetilde{\sum_{j_2,n_\ell}} \triangleq \sum_{n_1=0}^{j_2} \sum_{n_2=0}^{n_1} \cdots \sum_{n_{m_2-1}=0}^{n_{m_2-2}} \frac{j_2!}{(n_{m_2-1})!} \prod_{t=1}^{m_2-1} \frac{(t!)^{n_{t+1}-n_t}}{(n_{t-1}-n_t)!}$, $n_0 = j_2$, $n_{m_2} = 0$, $\Phi_{n_\ell} = \sum_{\ell=1}^{m_2-1} n_\ell$, and $\Lambda(i_2, j_2, n_\ell, k_2) = (-1)^{i_2+j_2}\binom{N-n}{i_2}\binom{n+i_2-1}{j_2}\binom{m_2+\Phi_{n_\ell}-1}{k_2}$. Moreover, $\Gamma(\cdot)$ is the Gamma function [35], and $K_v(\cdot)$ denotes the vth-order modified Bessel function of the second kind [35].

Proof: Please see Appendix A for the proof. ■

C. ASYMPTOTIC OP

In order to gain more engineering insights, we now consider the asymptotic behavior of OP at high SNRs.

Corollary 1: In the high SNR regime, i.e., $\rho \to \infty$, the asymptotic OP at D_n is derived as

$$P_{out}^{n} \approx \begin{cases} \frac{(m_1/\Omega_1)^{m_1}}{m_1!}\left(\frac{d_2 \varepsilon_n^*}{\rho}\right)^{m_1} \\ + \frac{N!(m_2!)^{-n}}{(N-n)!n!}\left(\frac{m_2 d_1 \varepsilon_n^*}{\Omega_2 \rho}\right)^{m_2 \cdot n}, & \widehat{R}_k < \widehat{R}_k^{up} \\ 1, & \widehat{R}_k \geq \widehat{R}_k^{up}, \end{cases} \quad (19)$$

which reveals that a diversity order of $\min(m_1, nm_2)$ is achieved at D_n when $\widehat{R}_k < \widehat{R}_k^{up}$ with $1 \leq k \leq n \leq N$.

Proof: Please see Appendix B. ■

Remark 2 (OP of Ideal Hardware): By setting $d_0 = 0$ and $d_1 = d_2 = 1$, the exact and asymptotic expressions of P_{out}^{n} in (18) and (19) reduce to their respective ideal-case forms, i.e., [14, eqs. (20) and (26)].

D. IMPACT OF RHI ON OP

Comparing (12) and (13), an important observation is that $\widehat{R}_k^{up} < \widehat{R}_{k,id}^{up}$. That is, the existence of RHI results in a lower upper bound on D_k's target rate $\widehat{R}_k$ compared to that in ideal NOMA. In this context, we consider the following three cases to separately analyze the impact of RHI on P_{out}^{n}.

- Consider the case $\widehat{R}_k < \widehat{R}_k^{up} < \widehat{R}_{k,id}^{up}$. In this case, (19) reveals that D_n in NOMA with RHI achieves the same diversity order of $\min(m_1, nm_2)$ as that in NOMA without RHI.[3] However, RHI degrades D_n's outage performance. Intuitively, it is easy to see from (5) that the achievable SINR for D_n to detect D_k's message is lower than that in ideal NOMA systems. Mathematically, the decreasing in the upper bound of D_k's target rate results in an increasing[4] in ε_n^*, thus increasing P_{out}^{n} in (19).
- Consider the case $\widehat{R}_k^{up} \leq \widehat{R}_k < \widehat{R}_{k,id}^{up}$. As shown in (18) and (19), $P_{out}^{n} = 1$ if $\widehat{R}_k \geq \widehat{R}_k^{up}$. However, since

[3] It is well-know that the external-user interference(s) (usually called CCI) will result in a non-zero outage floor at the receiver, i.e., no diveristy can be obtained, if the power of CCI is proportional to the transmit power [28]. This is because the CCI received at the receiver comes from a *different* fading channel with that of the desired singal at the reciever, then it unavoidably reflects an outage floor at the receiver. On the other hand, in NOMA-based networks or conventional dual-hop relaying networks with RHI, the distortion noises induced by RHI or the singals of all stronger users (i.e., IUIs) also show up interference terms that are proportional to the transmit power, while they go through *the same channel* as the desired signal at the receiver. Therefore, diversity order is maintained if the following *critical* condition is satisfied: the target rate of the receiver is chosen to be lower than its upper bound, which depends on the PA coefficients [3], [14] or hardware impairments levels [25]. Otherwise, the OP equals to 1 (i.e., outage floor). So, in a sense, the outage floor still exists in NOMA or hardware-impaired systems due to IUIs or RHI, since it cannot be crossed by simply increasing the transmit power.

[4] From (12), we have $\alpha_k/(\sum_{j=k+1}^{N} \alpha_j + d_0) = 2^{2\widehat{R}_k^{up}} - 1$ for $1 \leq k \leq n \leq N-1$. Thus, we can rewrite ε_k as $\varepsilon_k = \frac{1}{\alpha_k} \frac{(2^{2\widehat{R}_k^{up}}-1)(2^{2\widehat{R}_k}-1)}{(2^{2\widehat{R}_k^{up}}-1)-(2^{2\widehat{R}_k}-1)}$. Noting that ε_k is a monotone decreasing function of $\widehat{R}_k^{up}$. Hence, an decreasing in ε_k will lead to an increasing in ε_k, thus increasing $\varepsilon_n^* = \max\{\varepsilon_1, \cdots, \varepsilon_n\}$.

$\widehat{R}_k < \widehat{R}^{up}_{k,id}$, the OP of D_n in NOMA without RHI still experiences a diversity order of $\min(m_1, nm_2)$. Therefore, RHI will make D_n be in full outage state, i.e., $P^n_{out} = 1$, at smaller target rate upper bounds compared to the ideal scenario.

- Consider the case $\widehat{R}_k \geq \widehat{R}^{up}_{k,id} > \widehat{R}^{up}_k$. In this case, either the ideal or hardware-impaired NOMA user goes into full outage state, irrespective the system parameters, such as system SNR, the fading parameters (m_1 and m_2), or number of users N, which is also clarified in Remark 1.

To sum up, the OP of the impaired NOMA system is more sensitive to the choice of system parameters, i.e., the PA coefficients and target rates, compared to the ideal NOMA system. All of the above observations are well illustrated and verified in Figs. 2 $\sim$ 4 in Section V.

IV. ERGODIC RATE

Like [3] and [14], we now consider the case where target rates of different users are opportunistically allocated based on their channel conditions, i.e., $\widehat{R}_n = R_n$. In this scenario, it can be verified from (5) and (8) that $R_{k\to n} > \widehat{R}_k = R_k$ always holds since $|h_{2,n}|^2 \geq |h_{2,k}|^2$ for $k < n \leq N$ [3]. Therefore, all users can be served with zero outage probability but with different data rates. According to (6), (7), and (9), the exact individual ergodic rate (IER) at D_n can be expressed by

$$R^n_{ave} = \frac{1}{2}\mathbb{E}\left[\log_2\left(1 + \frac{\alpha_n Z_n}{\tau_n Z_n + 1}\right)\right], \tag{20}$$

where $\tau_n = (\sum_{j=n+1}^{N}\alpha_j + d_0)$ for $1 \leq n \leq N-1$, and $\tau_N = d_0$. Accordingly, the system ESR can be expressed by

$$R^{sum}_{ave} = \sum\nolimits_{n=1}^{N} R^n_{ave}. \tag{21}$$

A. ACCURATE APPROXIMATIONS OF IER AND ESR

The IER at D_n in (20) can be rewritten as

$$\begin{aligned} R^n_{ave} &= \frac{1}{2}\mathbb{E}\left[\log_2\left(\frac{1 + (\alpha_n + \tau_n)Z_n}{1 + \tau_n Z_n}\right)\right] \\ &\triangleq \overline{C}_n(\alpha_n + \tau_n) - \overline{C}_n(\tau_n), \end{aligned} \tag{22}$$

where $\overline{C}_n(\lambda)$ is defined as

$$\overline{C}_n(\lambda) \triangleq \frac{1}{2}\mathbb{E}\left[\log_2(1 + \lambda Z_n)\right], \ \lambda > 0. \tag{23}$$

Unfortunately, it is not easily tractable to get an exact closed-form expression of $\overline{C}_n(\lambda)$. Alternatively, using the Taylor expansion of the function $\log_2(1 + \lambda Z_n)$ about the mean of λZ_n, i.e., $\mathbb{E}[\lambda Z_n]$, we can give an analytical tight approximation to $\overline{C}_n(\lambda)$ as [31]

$$\begin{aligned} \overline{C}_n(\lambda) &\approx \frac{\ln(1 + \mathbb{E}[\lambda Z_n])}{2\ln(2)} - \frac{\mathbb{E}[(\lambda Z_n)^2] - \mathbb{E}^2[\lambda Z_n]}{4\ln(2)(1 + \mathbb{E}^2[\lambda Z_n])^2} \\ &= \frac{\ln(1 + \lambda\mathbb{E}[Z_n])}{2\ln(2)} - \lambda^2\frac{\mathbb{E}[(Z_n)^2] - \mathbb{E}^2[Z_n]}{4\ln(2)(1 + \lambda^2\mathbb{E}[Z_n])^2}. \end{aligned} \tag{24}$$

To evaluate (24), we need to derive closed-form solution for the generalized higher moments of Z_n, which can be given by

$$\mathbb{E}[Z^\mu_n] = \int_0^\infty z^\mu f_{Z_n}(z)\mathrm{d}z, \ \mu \geq 1. \tag{25}$$

Lemma 1: The μ^{th}-order moment of Z_n is given by

$$\begin{aligned} &\mathbb{E}[Z^\mu_n] \\ &= \frac{\mu Q_n}{\Gamma(m_2)}\sum_{i_1=0}^{m_1-1}\sum_{j_1=0}^{i_1}\sum_{i_2=0}^{N-n}\sum_{j_2=0}^{n+i_2-1}\sum_{j_2,n_\ell}^{\sim}\sum_{k_2=0}^{m_2+\Phi_{n_\ell}-1} \\ &\times \sum_{q=0}^{k_2+j_1+2}\frac{\binom{i_1}{j_1}\binom{k_2+j_1+2}{q}}{i_1!}\Lambda(i_2, j_2, n_\ell, k_2) \\ &\times(\beta_1)^{i_1}\left(\frac{\beta_2}{j_2+1}\right)^{m_2+\Phi_{n_\ell}}\left(\frac{\beta_1 d_1}{\beta_2 d_2}\right)^{\frac{k_2-j_1+1}{2}} \\ &\times c^q(-1)^{i_1+m_2+\Phi_{n_\ell}+\mu-q}\frac{\partial^{i_1+m_2+\Phi_{n_\ell}+\mu-q}\Upsilon(s)}{\partial s^{i_1+m_2+\Phi_{n_\ell}+\mu-q}}\Big|_{s=\beta_1+\beta_2}, \end{aligned} \tag{26}$$

where

$$\begin{aligned} \Upsilon(s) = &\frac{\Gamma(k_2+2)\,\Gamma(j_1+1)}{2c\sqrt{\beta_1\beta_2}e^{-sc/2}} \\ &\times W_{-\frac{k_2+j_1+2}{2},\frac{k_2-j_1+1}{2}}\left(\frac{c(s+\sqrt{s^2-4\beta_1\beta_2})}{2}\right) \\ &\times W_{-\frac{k_2+j_1+2}{2},\frac{k_2-j_1+1}{2}}\left(\frac{c(s-\sqrt{s^2-4\beta_1\beta_2})}{2}\right). \end{aligned} \tag{27}$$

In (26), the notation $\frac{\partial^n f(x)}{\partial x^n}$ denotes the n-th order derivative of $f(x)$ with respect to x. Note that $\frac{\partial^0 f(x)}{\partial x^0} = f(x)$. Moreover, in (27), $c = \frac{1}{d_1 d_2}$, $\beta_1 = \frac{m_1 d_2}{\Omega_1 \rho}$, and $\beta_2 = \frac{(j_2+1)m_2 d_1}{\Omega_2 \rho}$, and $W_{a,b}(\cdot)$ denotes the Whittaker function [35].

Proof: Please see Appendix C. ∎

It is worth noting that although (26) appears complicated, it is in closed-form since higher order derivatives of arbitrary order are known for the Whittaker function [25], [34]. Therefore, (26) can be analytically evaluated in an efficient way. The numerical results in this paper were produced by using the Symbolic Math Toolbox in MATLAB.

Tight analytical closed-form expressions for the IER and system ESR are summarized in the following theorem.

Theorem 2: The IER of the NOMA-based AF relaying network suffering from RHI can be tightly approximated as follows

$$\begin{aligned} R^n_{ave} \simeq R^{n,apx}_{ave} \triangleq &\frac{1}{2\ln(2)}\ln\left(\frac{1 + (\alpha_n + \tau_n)\mathbb{E}[Z_n]}{1 + \tau_n\mathbb{E}[Z_n]}\right) \\ &- \frac{(\alpha_n + \tau_n)^2(\mathbb{E}[(Z_n)^2] - \mathbb{E}^2[Z_n])}{4\ln(2)(1 + (\alpha_n + \tau_n)^2\mathbb{E}[Z_n])^2} \\ &+ \frac{(\tau_n)^2(\mathbb{E}[(Z_n)^2] - \mathbb{E}^2[Z_n])}{4\ln(2)(1 + (\tau_n)^2\mathbb{E}[Z_n])^2}. \end{aligned} \tag{28}$$

With (28), the system ESR can be approximated as

$$R_{ave}^{sum} \simeq R_{ave}^{sum,aprx} \triangleq \sum_{n=1}^{N} R_{ave}^{n,apx}, \tag{29}$$

Proof: Substituting (24) into (22), we get (28), where $\mathbb{E}[Z_n]$ and $\mathbb{E}[Z_n^2]$ can be obtained by invoking $\mu = 1$ and $\mu = 2$ into (26), respectively. Accordingly, a tight analytical expression for the ESR in (29) can be derived directly. ■

Remark 3: Theorem 2 provides unified approximated expressions for the IER and ESR of NONMA-based AF networks with and without RHI, which will be proved to be highly accurate. The results in (28) and (29) are new, and have not been reported. In particular, for the special case of ideal hardware as considered in [14], tight analytical expressions of IER and ESR can be obtained by substituting $d_0 = 0$ and $d_1 = d_2 = 1$ into (28) and (29), respectively.

B. ASYMPTOTIC ANALYSIS OF IER AND ESR

We now turn our attention to the ergodic rate in the high SNR regime. However, it is difficult to obtain the asymptotic expressions of IER and ESR from (28) and (29). To solve this issue, we first apply the approximation[5] $\mathbb{E}[\log_2(1 + x/y)] \approx \log_2(1 + \mathbb{E}[x]/\mathbb{E}[y])$, which is introduced in [24, eq. (35)], to approximate R_{ave}^n in (22) as

$$R_{ave}^n \approx \frac{1}{2}\log_2\left(1 + \frac{\alpha_n \mathbb{E}\{XY_n\}}{\tau_n \mathbb{E}\{XY_n\} + d_1\mathbb{E}\{X\} + d_2\mathbb{E}\{Y_n\} + 1}\right). \tag{30}$$

To evaluate (30), we need closed-form expressions for $\mathbb{E}\{X\}$, and $\mathbb{E}\{Y_n\}$. $\mathbb{E}\{X\}$ can be obtained from the definition of the Nakagami-m PDF according to $\mathbb{E}\{X\} = \rho\mathbb{E}\{|h_1|^2\} = \Omega_1\rho$. In addition, $\mathbb{E}\{Y_n\}$ can be calculated by

$$\mathbb{E}\{Y_n\} = \int_0^\infty y f_{Y_n}(y)\mathrm{d}y \tag{31}$$

Invoking the PDF $f_{Y_n}(y)$ in (48) into (31) and then using [36, eq. (3.385.3)], it can be shown that $\mathbb{E}\{Y_n\} = \rho\Omega_{2n}$, where $\Omega_{2n} = \Omega_2\varpi(n)$, and

$$\varpi(n) = Q_n \sum_{i_2=0}^{N-n} \sum_{j_2=0}^{n+i_2-1} \widetilde{\sum_{j_2,n_\ell}} \frac{\delta_1(i_2,j_2)\Gamma(m_2 + \Phi_{n_\ell} + 1)}{\Gamma(m_2+1)(j_2+1)^{m_2+\Phi_{n_\ell}+1}}. \tag{32}$$

Putting the above results into (30) and after some manipulations, a simple approximate expression for the IER of D_n $(1 \le n \le N)$ with RHI is given by

$$R_{ave}^n \approx \frac{1}{2}\log_2\left(1 + \frac{\alpha_n\Omega_1\Omega_{2n}\rho^2}{\tau_n\Omega_1\Omega_{2n}\rho^2 + (d_1\Omega_1 + d_2\Omega_{2n})\rho + 1}\right). \tag{33}$$

[5] In fact, the asymptotic IER/ESR of the hardware-impaired system can be straightforwardly obtained from (20) by assuming $\rho \to \infty$. The main purpose of using this approximation method herein is to derive the asymptotic expressions for the IER of D_N and system ESR of ideal hardware system.

Moreover, by substituting $d_0 = 0$ and $d_1 = d_2 = 1$ into (33), an approximate expression for the IER of D_n $(1 \le n \le N-1)$ without RHI by can be obtained as

$$R_{ave,id}^n \approx \frac{1}{2}\log_2\left(1 + \frac{\alpha_n\Omega_1\Omega_{2n}\rho^2}{\sum_{j=n+1}^{N}\alpha_j\Omega_1\Omega_{2n}\rho^2 + (\Omega_1+\Omega_{2n})\rho + 1}\right). \tag{34}$$

Besides, IER of D_N without RHI is approximated by

$$R_{ave,id}^N \approx \frac{1}{2}\log_2\left(1 + \frac{\alpha_N\Omega_1\Omega_{2N}\rho^2}{(\Omega_1+\Omega_{2N})\rho + 1}\right). \tag{35}$$

From (33), (34), and (35), we can obtain asymptotic high-SNR IER and ESR expressions for NOMA-based AF networks with and without RHI in what follows.

Corollary 2: When $\rho \to \infty$, the asymptotic expression for IER of NOMA-based AF networks with and without RHI are respectively given by

$$R_{ave}^n \approx \begin{cases} \frac{1}{2}\log_2\left(1 + \frac{\alpha_n}{\sum_{j=n+1}^{N}\alpha_j + d_0}\right), & 1 \le n < N \\ \frac{1}{2}\log_2\left(1 + \frac{\alpha_N}{d_0}\right), & n = N. \end{cases} \tag{36}$$

$$R_{ave,id}^n \approx \begin{cases} \frac{1}{2}\log_2\left(1 + \frac{\alpha_n}{\sum_{j=n+1}^{N}\alpha_j}\right), & 1 \le n < N \\ \frac{1}{2}\log_2\left(1 + \frac{\alpha_N\Omega_1\Omega_{2N}}{\Omega_1+\Omega_{2N}}\rho\right), & n = N. \end{cases} \tag{37}$$

Accordingly, the asymptotic ESR of NOMA-based AF networks with and without RHI are respectively given by

$$R_{ave}^{sum} \approx \frac{1}{2}\log_2\left(1 + \frac{1}{d_0}\right). \tag{38}$$

$$R_{ave,id}^{sum} \approx \frac{1}{2}\log_2\rho + \frac{1}{2}\log_2\left(\frac{\Omega_1\Omega_{2N}}{\Omega_1+\Omega_{2N}}\right). \tag{39}$$

Proof: Please see Appendix D. ■

C. THE EFFECT OF RHI ON IER AND SYSTEM ESR

1) THE EFFECT OF RHI ON IER

Firstly, consider the user D_n $(1 \le n \le N-1)$. We see from (36) and (37) that there exists an IER ceiling in the high-SNR regime irrespective of channel conditions (i.e., m_i and Ω_i, $i = 1, 2$) and N. Noting that the IER ceiling of D_n with RHI is attributed to the combined effect of RHI and IUIs from all stronger users, while the IER ceiling of D_n in the ideal case is resulted from the IUIs only. Moreover, comparing (36) and (37), it is clear that RHI has a detrimental effect on the asymptotic IER in terms of decreasing the IER ceiling. Secondly, consider the IER of the user D_N with the best channel gain. As shown in (37), the asymptotic IER of D_N without RHI goes unboundedly as ρ increases since it is free from IUI, thus playing a dominate role in the asymptotic system ESR. However, the IER of D_N with RHI in (36) is a constant due to the additive effect of RHI.

2) THE EFFECT OF RHI ON ESR

The asymptotic ESR without RHI scales as $\frac{1}{2}\log_2\rho$ as revealed in (39), thus growing unboundedly as $\rho \to \infty$. Intuitively, this is because the asymptotic ESR in the ideal scenario is dominated by the IER of the best user D_N, as explained above. However, from (38), we observe that the asymptotic ESR with RHI saturates in the high-SNR regime, which is dependent only on the RHI levels, i.e., d_0. Therefore, RHI has a substantial impact on ESR, especially when ρ is high.

D. ESR IN OMA-BASED RELAYING SYSTEMS

For performance comparison, we consider the time division multiple access (TDMA) scheme in this subsection, which is a typical OMA scheme [6]. Note that the conventional OMA-based dual-hop relaying system using TDMA requires $N \times 2$ time slots to support N users, while NOMA-based dual-hop relaying system can support N users during 2 times slots as described in Section II-A. Thus, the achievable rate of D_n in OMA-based relaying system with RHI is given by

$$R_n^{OMA} = \frac{1}{N} \times \frac{1}{2}\log_2\left(1 + \frac{X\mathrm{Y}_n}{d_0 X\mathrm{Y}_n + d_1 X + d_2 \mathrm{Y}_n + 1}\right), \tag{40}$$

where $1 \le n \le N$, $X = \rho|h_1|^2$ and $\mathrm{Y}_n = \rho|h_{2,n}|^2$.

From (40), the ESR of the OMA-based relaying system with RHI is given by

$$R_{ave}^{sum,OMA} = \mathbb{E}\left\{\sum_{n=1}^{N} R_n^{OMA}\right\}. \tag{41}$$

Note that we can use (41) to obtain the ESR achieved by the OMA-based relaying system with and without RHI. Then these results can be used as benchmarks to compare with the NOMA-based relaying systems in the next section.

More importantly, when $\rho \to \infty$, it is easy to observe from (40) that

$$R_n^{OMA} \approx \frac{1}{N} \times \frac{1}{2}\log_2\left(1 + \frac{1}{d_0}\right). \tag{42}$$

Substituting (42) into (41), yields

$$R_{ave}^{sum,OMA} \approx \frac{1}{2}\log_2\left(1 + \frac{1}{d_0}\right). \tag{43}$$

From (38) and (43), we find that under the impact of RHI, the asymptotic ESR in the NOMA-based relaying system is the same as that in the OMA-based relaying system, both of which are only depended on the RHI level, i.e., d_0.

V. NUMERICAL RESULTS

This section presents a set of Monte-Carlo simulations to validate the theoretical results. The simulation results are obtained by performing 10^6 random channel realizations. Without loss of generality, we set the power allocation factors as [3], [14] $\alpha_n = \frac{N-n+1}{\mu}$, where $\mu = \frac{N(N+1)}{2}$ is to ensure $\sum_{n=1}^{N}\alpha_n = 1$. Moreover, like [25] and [28], we assume that the $S \to R$ and $R \to D_n$ links have the same impairment level, i.e., $\kappa \triangleq \kappa_{SR} = \kappa_{RD}$. As such, we have $d_0 = \kappa^4 + 2\kappa^2$ and $d_1 = d_2 = 1 + \kappa^2$. Besides, the unit of target rate is bps/Hz and is omitted in the following analysis for simplicity.

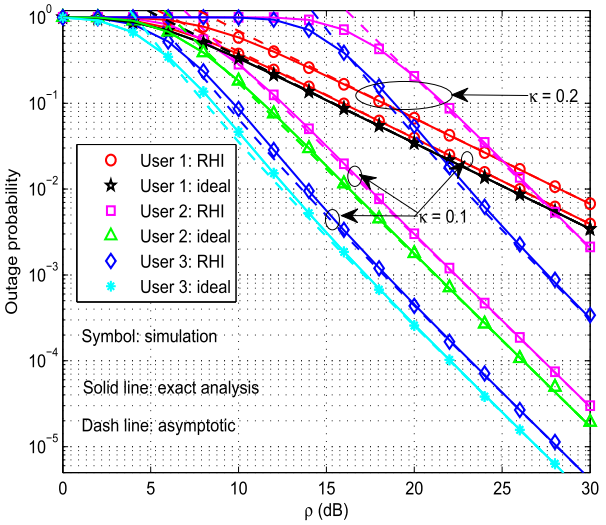

FIGURE 2. OP vs. SNR ρ : $\kappa = \{0.1, 0.2\}$, $m_1 = 2$, $m_2 = 1$, $\Omega_1 = 10$, $\Omega_2 = 5$, and $N = 3$ with $\alpha_n = \{1/2, 1/3, 1/6\}$ and $\widehat{R}_n = \{0.4, 0.6, 0.7\}$ bps/Hz for $n = 1, 2, 3$.

A. EFFECT OF RHI ON OP

In Fig. 2, the outage probability with or without RHI is plotted as a function of system SNR ρ. Herein, we plot curves for two different values of RHI levels: $\kappa \in \{0.1, 0.2\}$. Moreover, we consider the case of three users by setting $N = 3$, where the power coefficients are $\alpha_1 = 1/2$, $\alpha_2 = 1/3$, and $\alpha_3 = 1/6$. With these settings, the value of $\widehat{R}_n^{up}$ (i.e., the upper bound of D_n's target rate) can be computed by (12) and (15), where $n = 1, 2, 3$. Specifically, we get $\widehat{R}_n^{up} \approx \{0.49, 0.74, 1.61\}$ for a low level of impairments of $\kappa = 0.1$, and $\widehat{R}_n^{up} \approx \{0.45, 0.615, 0.8\}$ for a high level of impairments of $\kappa = 0.2$ [25]–[30]. Furthermore, we set the target rates as $\widehat{R}_n = \{0.4, 0.6, 0.7\}$ so as $\widehat{R}_n < \widehat{R}_n^{up}$, which holds in both hardware-impaired cases ($\kappa = 0.1$ and 0.2). From Fig. 2, we observe that exact analytical and simulation results match well over the entire SNR range, and the asymptotic results are very tight at high SNRs. Moreover, it can be verified that D_n in NOMA with RHI achieves the same diversity order of $\min(m_1, m_2\, n)$ as that in the ideal hardware scenario when $\widehat{R}_n < \widehat{R}_n^{up}$, which is proved by (19). However, as shown in Fig. 2, the existence of RHI degrades the user's outage performance. In particular, as the impairment level κ increases from 0.1 to 0.2, the performance loss compared to the ideal-hardware case, increases substantially when ρ is large.

More detailed effects of RHI on OP are illustrated in Fig. 3. We first focus on the outage performance of D_2. In agreement with the analysis in Section III-D (the first case), it can be seen from the curves of Case 1 that a diversity of

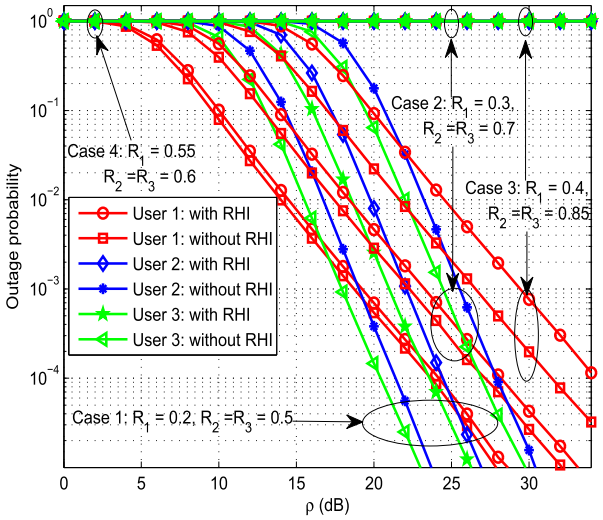

FIGURE 3. OP vs. SNR ρ when $m_1 = 4$, $m_2 = 2$, $\Omega_1 = \Omega_2 = 1$, $\kappa = 0.2$, and $N = 3$ with $\alpha_1 = 1/2$, $\alpha_2 = 1/3$, and $\alpha_3 = 1/6$. The target rate upper bounds are $\widehat{R}_n^{up} \approx \{0.45, 0.615, 0.8\}$.

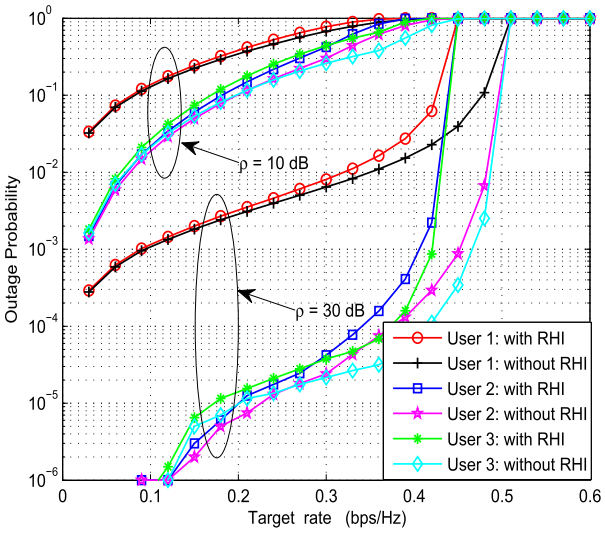

FIGURE 4. OP vs. target rate when $m_1 = 2$, $m_2 = 1$, $\Omega_1 = \Omega_2 = 1$, $\kappa = 0.2$, and $N = 3$ with $\alpha_1 = 1/2$, $\alpha_2 = 1/3$, and $\alpha_3 = 1/6$. The target rate upper bounds are $\widehat{R}_n^{up} \approx \{0.45, 0.615, 0.8\}$.

$\min(4, 2 \times 2) = 4$ is obtained at D_2 with or without RHI when $\widehat{R}_2 < \widehat{R}_2^{up} < \widehat{R}_{2,id}^{up}$, where $\widehat{R}_2 = 0.5$, $\widehat{R}_2^{up} \approx 0.615$, and $\widehat{R}_{2,id}^{up} \approx 0.8$. However, we observe from Case 2 in Fig. 3 that D_2 in NOMA with RHI is in full outage over the entire SNR range, i.e., $P_{out}^2 = 1$, whereas a diversity order of 4 is still obtained at D_2 in the ideal scenario, due to the fact that the condition $\widehat{R}_2^{up} < \widehat{R}_2 = 0.7 < \widehat{R}_{2,id}^{up} \approx 0.8$ holds in Case 2. In addition, we see from Case 3 of Fig. 3 that D_2 in NOMA with and without RHI are always outage when $\widehat{R}_2^{up} < \widehat{R}_{2,id}^{up} < \widehat{R}_2 = 0.85$. These observations observed from Cases 2 and 3 of Fig. 3 are concurred with the conclusions of the second and third cases drawn in Section III-D, respectively.

Furthermore, we observe from Fig. 3 that all users in NOMA with RHI go into the full outage states in Case 4, where we set $\widehat{R}_1 = 0.55$. Since $\widehat{R}_1 > \widehat{R}_1^{up} \approx 0.45$, it is impossible for D_1 to detect its own message. Thus, as explained in Remark 1, both stronger users D_2 and D_3 cannot detect D_1's message before detecting their desired messages if $\widehat{R}_1 > \widehat{R}_1^{up}$, which lead to the implementation failure of SIC. As a result, outages will also be declared at D_2 and D_3. Similarly, we see from Case 4 in Fig. 3 that all users in ideal-hardware NOMA system are always in outage due to the fact that $\widehat{R}_1 = 0.55 > \widehat{R}_{1,id}^{up} \approx 0.5$. Besides, by comparing the OP curves of D_1 in Cases 1, 2, and 3, we find that the performance loss caused by RHI increases substantially as the target rate increases, which is in line with [25].

Figure. 4 plots the outage probability versus the target rate $\widehat{R}$ for $\rho = 10$ dB and $\rho = 30$ dB. For the sake of brevity in interpretation, we assume $\widehat{R}_1 = \widehat{R}_2 = \widehat{R}_3 = \widehat{R}$. From Fig. 4, we observe that the impact of RHI is neglectable at low target rates and/or low SNR (10 dB). Nevertheless, the impact of RHI becomes much greater as the target rate gets higher in the high SNR (30 dB) case, which is also illustrated in Fig. 3 (see the OP curves of D_1 in Cases 1, 2, and 3). Another important observation is that a target rate wall (upper bound) is created by IUIs in the ideal-hardware system, which cannot be crossed by simply increasing the SNR, whereas in presence of RHI, the value of the wall is decreased due to additive effect of RHI. Thus, we see that as $\widehat{R}$ increases, the hardware-impaired NOMA user goes into the full outage state much faster than the user in the ideal hardware system.

To sum up, from Figs. 2, 3, and 4, we confirm that the presence of RHI has a deleterious effect on the outage performance. Specifically, the detrimental effect of RHI becomes more prominent as the impairment level κ or/and target rates increase, especially in the high SNR regime. Particularly, the outage performance of NOMA with RHI is more sensitive to the choice of the power coefficients α_n and target rates $\widehat{R}_n$ compared to the ideal-hardware system.

B. EFFECT OF RHI ON ERGODIC RATES

In Fig. 5, we investigate the impact of RHI on the IERs and system ESR. With loss of any generality, we consider the two-user case by setting $N = 2$ for clearness. Fig. 5 confirm that IER or ESR is only sightly degraded by RHI at the low SNRs, but the performance loss induced by RHI increases substantially as ρ gets higher. More precisely, while the IER of weaker user D_1 gets saturated after a certain value of ρ in the absence of RHI, a lower IER ceiling of D_1 in the presence of RHI is observed due to the additive effect of RHI. Moreover, it can be seen that IER of the stronger user D_2 with RHI does not grow unboundedly as ρ increases, as is the case for D_2 without RHI. In this context, we observe from Fig. 5 that the asymptotic high-SNR ESR of the ideal hardware system scales as $\frac{1}{2}\log_2 \rho$ as revealed in (39), thus increasing no bound as ρ increases, whereas the ESR with RHI saturates at high SNRs, which is consistent to (38).

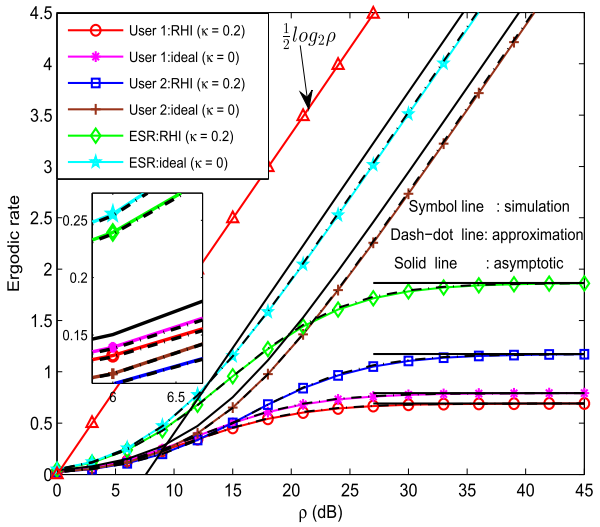

FIGURE 5. Ergodic rate vs. SNR ρ when $m_1 = m_2 = 2$, $\Omega_1 = 5$, $\Omega_2 = 1$, $\kappa = 0.2$, and $N = 2$ with $\alpha_1 = 2/3$, $\alpha_2 = 1/3$.

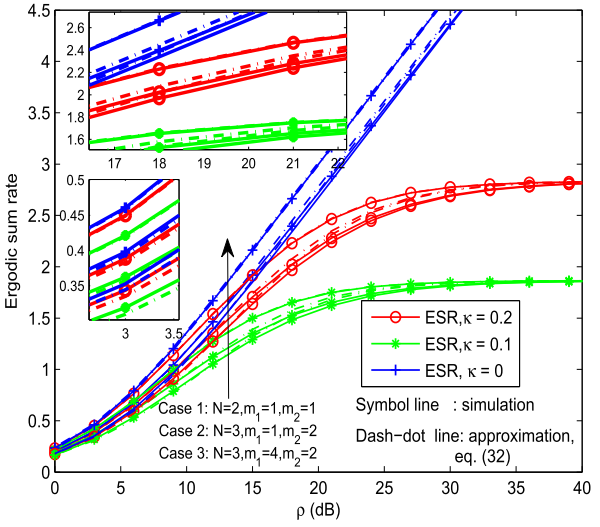

FIGURE 6. Ergodic sum rate vs. SNR ρ when $\Omega_1 = 1$, $\Omega_2 = 2$, $\kappa = \{0.1, 0.2\}$. For $N = 2$, $\alpha_1 = 2/3$ and $\alpha_2 = 1/3$. For $N = 3$, $\alpha_1 = 1/2$, $\alpha_2 = 1/3$, and $\alpha_3 = 1/6$.

In Fig. 6, we compare the system ESR of NOMA with and without RHI under different system configurations. From the figure, it can be shown that the ESR of ideal-hardware system monotonically increases with ρ and it can be enhanced as users' number or/and[6] the fading severity increase (i.e., N or/and m_i increases, $i = 1, 2$). Similar observations are also observed for the ESR of the hardware-impaired system in the low-to-medium SNR regions, whereas at high SNRs, the ESR saturates and approaches $\frac{1}{2}\log_2\left(1 + d_0^{-1}\right)$ as proved by (38). Therefore, unlike the ideal scenario, the benefit offered to the ESR by increasing m_i or/and N vanishes at the high SNRs, due to the presence of RHI. In addition, as the ESR ceiling is depended merely on the impairment levels κ, it decreases when κ is increased. In particular, it can be observed that with the increase in the value of impairments, the saturation point appears earlier, i.e., at the lower values of ρ.

It is worth noting that the provided simulation results shown in Fig. 5 and Fig. 6 match very well with the approximation results of (28) or (29) over the entire SNR range and in all considered scenarios, except for a small difference in sever fading environments,[7] i.e., when $m_i = 1$, $i = 1, 2$. Moreover, the asymptotic IER in (36) and ESR in (38) very tightly follows the analytical results at high enough SNR values.

Fig. 7 presents the ESR comparison of NOMA and OMA systems in the presence and the absence of RHI. It is observed

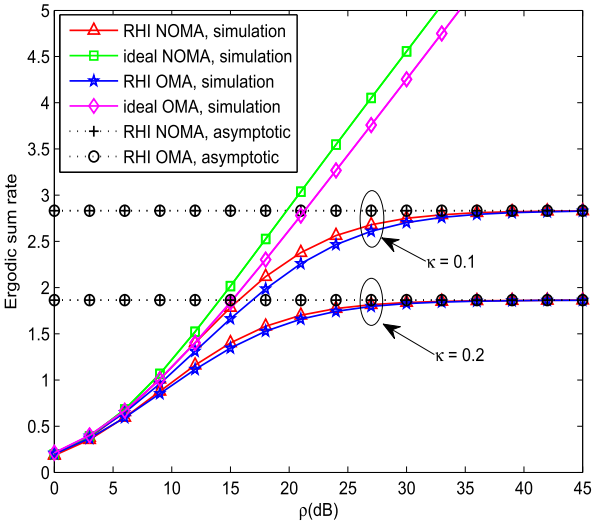

FIGURE 7. ESR comparison between NOMA and OMA with/without RHI, where $\Omega_1 = 1$, $\Omega_2 = 2$, $m_1 = 2$, $m_2 = 1$, $\kappa = \{0.1, 0.2\}$, and $N = 3$ with $\alpha_1 = 1/2$, $\alpha_2 = 1/3$, and $\alpha_3 = 1/6$.

from Fig. 7 that, in the absence of RHI, the ESR in either the NOMA system or the OMA system increases monotonically with the increase of ρ. In particular, the ESR of NOMA-based system outperforms that of the OMA-based one at moderate-to-high SNRs, which demonstrates the benefits of NOMA transmission. However, the presence of RHI causes ESR saturation phenomena at high SNRs in both systems. Since the ESR saturation value is only depended by the RHI levels, as revealed in (38) and (43), the asymptotic ESR curves of NOMA and OMA systems are overlapped together. In other words, the superiority of NOMA over OMA in terms of ESR disappears in the high SNR regimes, due to the presence of RHI. However, NOMA can provide better

[6]The ideal ESR curves of cases 1 and 2 are overlapped at high SNRs. This is because the asymptotic ESR is dominated by the capacity of D_N, which is restricted by the weaker link between $S \to R$ and $R \to D_N$.

[7]The high accuracy of the proposed analysis lies in the fact that the second order Taylor series approximation method is adopted. This method has been widely used in the ergodic capacity analysis of AF relaying systems subject to Nakagami-m fading, and its highly accurate have been well verified specifically for the moderate and high multipath fading environments, i.e., $m_i \geq 2$. In severe multipath fading environments, i.e., when $m_i < 2$, a slight discrepancy between the approximated and exact result is observed when this approach is employed. For more specific details about these observations, please refer to [31, Fig. 1], and references therein.

spectral efficiency and user fairness as more users are served at the same time, frequency, and spreading code [2], [3], [14].

VI. CONCLUSION

This paper investigated analytically the impact of residual hardware impairment (RHI) on the NOMA-based AF relaying network. Closed-form analytical and high-SNR asymptotic expressions for the outage probability (OP), individual ergodic rate (IER) and system ergodic sum rate (ESR) were obtained. Our theoretical analysis indicated that the outage performance is only sightly degraded by RHI at the low SNRs or/and at small target rates, but otherwise the outage performance loss can be very substantial. Furthermore, we observed that RHI has small impact on the capacity performance (i.e., IER and ESR) in the low SNR regime, but it becomes more influential as the SNR gets higher. In particular, while the ideal ESR in NOMA or OMA system without RHI grows unboundedly with SNR, the ESR with RHI approaches a deterministic value that is depended only on the hardware impairment levels. More importantly, at high SNRs, the advantage of NOMA over conventional OMA in terms of ESR for the ideal-hardware scenario no longer exists in the hardware-impaired scenario. But the application of NOMA in AF relaying networks still has its benefits. In particular, it can offer better spectral efficiency and user fairness, as compared to OMA.

APPENDIX A
PROOF OF THEOREM 1

A. STATISTICAL CHARACTERIZATIONS

Recall that $X = \rho|h_1|^2$ and $Y_n = \rho|h_{2n}|^2$. Since $|h_1|^2$ follows Gamma distribution, the probability density function (PDF) and the CDF of X are respectively given by

$$f_X(x) = \frac{m_1^{m_1} x^{m_1-1}}{(\rho\Omega_1)^{m_1}\Gamma(m_1)} e^{-\frac{m_1}{\rho\Omega_1}x}, \tag{44}$$

and

$$\begin{aligned} F_X(x) &= 1 - \frac{\Gamma(m_1, \frac{m_1 x}{\rho\Omega_1})}{\Gamma(m_1)} \\ &= 1 - e^{-\frac{m_1 x}{\rho\Omega_1}} \sum_{i_1=0}^{m_1-1} \frac{\left(\frac{m_1 x}{\rho\Omega_1}\right)^{i_1}}{i_1!}, \end{aligned} \tag{45}$$

where $\Gamma(\cdot,\cdot)$ represent the upper incomplete gamma function [35, eq. (8.350.2)].

Similarly, the PDF and CDF of *unordered* variable $\widetilde{Y}_n = \rho|\widetilde{h}_n|^2$ are respectively given by

$$f_{\widetilde{Y}_n}(y) = \frac{m_2^{m_2} y^{m_2-1}}{(\rho\Omega_2)^{m_2}\Gamma(m_2)} e^{-\frac{m_2}{\rho\Omega_2}y}, \tag{46}$$

and

$$F_{\widetilde{Y}_n}(y) = 1 - e^{-\frac{m_2 y}{\rho\Omega_2}} \sum_{i=0}^{m_2-1} \frac{\left(\frac{m_2 y}{\rho\Omega_2}\right)^{i}}{i!}. \tag{47}$$

In (45) and (47), the assumption of integer shape parameters is made to facilitate the algebraic manipulations for Nakagami-m fading, otherwise the analysis will be very tedious. Furthermore, the FDF and CDF of the *nth ordered* variable $Y_n = \rho|h_n|^2$ are respectively given by [14]

$$f_{Y_n}(y) = Q_n \sum_{i_2=0}^{N-n} (-1)^{i_2} \binom{N-n}{i_2} f_{\widetilde{Y}_n}(y) \left[F_{\widetilde{Y}_n}(y)\right]^{n+i_2-1}, \tag{48}$$

and

$$F_{Y_n}(y) = Q_n \sum_{i_2=0}^{N-n} \frac{(-1)^{i_2}\binom{N-n}{i_2}}{n+i_2} \left[F_{\widetilde{Y}_n}(y)\right]^{n+i_2}, \tag{49}$$

where $Q_n = \frac{N!}{(N-n)!(n-1)!}$. Using the multinomial theorem, $f_{|Y_n|^2}(y)$ and $F_{Y_n}(y)$ are respectively derived as [14]

$$\begin{aligned} f_{Y_n}(y) = Q_n \sum_{i_2=0}^{N-n} \sum_{j_2=0}^{n+i_2-1} \widetilde{\sum_{j_2,n_\ell}} \frac{\delta_1(i_2,j_2)}{\Gamma(m_2)} \left(\frac{m_2}{\rho\Omega_2}\right)^{m_2+\Phi_{n_\ell}} \\ \times e^{-(j_2+1)\frac{m_2}{\rho\Omega_2}y} y^{m_2+\Phi_{n_\ell}-1}, \end{aligned} \tag{50}$$

$$F_{Y_n}(y) = Q_n \sum_{i_2=0}^{N-n} \sum_{j_2=0}^{n+i_2} \widetilde{\sum_{j_2,n_\ell}} \frac{\delta_2(i_2,j_2)}{i_2+n} e^{-j_2\frac{m_2 y}{\rho\Omega_2}} \left(\frac{m_2 y}{\rho\Omega_2}\right)^{\Phi_{n_\ell}}, \tag{51}$$

where $\widetilde{\sum_{j_2,n_\ell}} = \sum_{n_1=0}^{j_2}\sum_{n_2=0}^{n_1}\cdots\sum_{n_{m_2-1}=0}^{n_{m_2-2}} \frac{j_2!}{(n_{m_2-1})!}\prod_{t=1}^{m_2-1}\frac{(t!)^{n_{t+1}-n_t}}{(n_{t-1}-n_t)!}$, $\Phi_{n_\ell} = \sum_{\ell=1}^{m_2-1} n_\ell$, with $n_0 = j_2$ and $n_{m_2} = 0$, $\delta_1(i_2,j_2) = (-1)^{i_2+j_2}\binom{N-n}{i_2}\binom{n+i_2-1}{j_2}$ and $\delta_2(i_2,j_2) = (-1)^{i_2+j_2}\binom{N-n}{i_2}\binom{n+i_2}{j_2}$.

B. DERIVATION OF EQUATION (18)

Referring to (17), we see that the key task to derive $F_{Z_n}(\varepsilon_n^*)$. Recall that $Z_n = \frac{XY_n}{d_1X+d_2Y_n+1}$. Then, $F_{Z_n}(\varepsilon_n^*)$ can be calculated by

$$\begin{aligned} F_{Z_n}(\varepsilon_n^*) &= \Pr\left\{\frac{XY_n}{d_1X+d_2Y_n+1} < \varepsilon_n^*\right\} \\ &= \Pr\left\{(Y_n - d_1\varepsilon_n^*)X < d_2Y_n\varepsilon_n^* + \varepsilon_n^*\right\}. \end{aligned} \tag{52}$$

Considering two cases, i.e., $Y_n \le d_1\varepsilon_n^*$ and $Y_n > d_1\varepsilon_n^*$, and performing some algebraic manipulations, we obtain

$$\begin{aligned} F_{Z_n}(\varepsilon_n^*) &= \int_0^{d_1\varepsilon_n^*} f_{Y_n}(y)\mathrm{d}y + \int_{d_1\varepsilon_n^*}^{\infty} f_{Y_n}(y) F_X\left(\frac{d_2 y\varepsilon_n^* + \varepsilon_n^*}{y - d_1\varepsilon_n^*}\right)\mathrm{d}y \\ &= 1 - \int_{d_1\varepsilon_n^*}^{\infty}\left[1 - F_X\left(\frac{d_2 y\varepsilon_n^* + \varepsilon_n^*}{y - d_1\varepsilon_n^*}\right)\right] f_{Y_n}(y)\mathrm{d}y. \end{aligned} \tag{53}$$

Using the CDF of X in (45) and the PDF of Y_n in (50), we can evaluate (53) as

$$F_{Z_n}(\varepsilon_n^*) = 1 - Q_n \sum_{i_2=0}^{N-n} \sum_{j_2=0}^{n+i_2-1} \sum_{j_2,n_\ell}^{\sim} \frac{\delta_1(i_2,j_2)}{\Gamma(m_2)} \left(\frac{m_2}{\rho\Omega_2}\right)^{m_2+\Phi_{n_\ell}} \times \underbrace{\int_{d_1\varepsilon_n^*}^{\infty} e^{-(j_2+1)\frac{m_2}{\rho\Omega_2}y} y^{m_2+\Phi_{n_\ell}-1} \frac{\Gamma(m_1, \frac{m_1\varepsilon_n^*}{\rho\Omega_1}\frac{d_2 y+1}{y-d_1\varepsilon_n^*})}{\Gamma(m_1)} \mathrm{d}y}_{I}. \quad (54)$$

Applying [36, eq. (8.352.4)] and setting $t = y - d_1\varepsilon_n^*$, the integral I in (54) can be expressed as

$$I = e^{-\varepsilon_n^*\left(\frac{m_1 d_2}{\rho\Omega_1} + \frac{(j_2+1)m_2 d_1}{\rho\Omega_2}\right)} \sum_{i_1=0}^{m_1-1} \frac{(\frac{m_1\varepsilon_n^*}{\rho\Omega_1})^{i_1}}{i_1!} \times I_1, \quad (55)$$

where

$$I_1 = \int_0^{\infty} e^{-\frac{(j_2+1)m_2}{\rho\Omega_2}t - \frac{m_1\varepsilon_n^*}{\rho\Omega_1}\frac{d_1\, d_2\varepsilon_n^*+1}{t}} \times (t + d_1\varepsilon_n^*)^{m_2+\Phi_{n_\ell}-1} \left(d_2 + \frac{d_1\, d_2\varepsilon_n^*+1}{t}\right)^{i_1} \mathrm{d}t. \quad (56)$$

Using the binomial expansion for the powers of t, i.e., $(t + d_1\varepsilon_n^*)^{m_2+\Phi_{n_\ell}-1}$ and $(d_2 + \frac{d_1\, d_2\varepsilon_n^*+1}{t})^{i_1}$ within the integral, and then applying [35, eq. (3.471.9)], I_1 in (56) can be solved as

$$I_1 = \sum_{j_1=0}^{i_1} \sum_{k_2=0}^{m_2+\Phi_{n_\ell}-1} \binom{i_1}{j_1} \binom{m_2+\Phi_{n_\ell}-1}{k_2} (d_1 d_2\varepsilon_n^* + 1)^{j_1} \times (d_1\varepsilon_n^*)^{m_2+\Phi_{n_\ell}-k_2-1} \left(\frac{m_1\Omega_2\varepsilon_n^*(d_1 d_2\varepsilon_n^*+1)}{(j_2+1)m_2}\right)^{\frac{k_2-j_1+1}{2}} \times 2{d_2}^{i_1-j_1} K_{k_2-j_1+1} \left(\frac{2}{\rho}\sqrt{\frac{(j_2+1)m_1 m_2\varepsilon_n^*(d_1 d_2\varepsilon_n^*+1)}{\Omega_1\Omega_2}}\right). \quad (57)$$

As a result, the closed-form analytical expression of $F_{Z_n}(\varepsilon_n^*)$ can be found by substituting (55) with I_1 given in (57) into (54), resulting in (18).

APPENDIX B
PROOF OF COROLLARY 1

When $\rho \to \infty$, we have $\frac{x}{\rho} \to 0$. Therefore, the CDF of X in (45) can be approximated as

$$F_X(x) \approx \frac{(m_1/\Omega_1)^{m_1}}{m_1!}\left(\frac{x}{\rho}\right)^{m_1}. \quad (58)$$

Similarly, $F_{Y_n}(y)$ in (51) can be approximated as [14]

$$F_{Y_n}(y) \approx \frac{N!(m_2!)^{-n}}{(N-n)!n!}\left(\frac{m_2 y}{\Omega_2\rho}\right)^{m_2\cdot n}. \quad (59)$$

Now, we focus on deriving the asymptotic OP in high SNRs. By adopting the well-known inequality: $\frac{XY}{1+X+Y} \le \min(X, Y)$, Z_n can be upper bound Z_n as

$$Z_n \le \min\left(\frac{X}{d_2}, \frac{Y_n}{d_1}\right). \quad (60)$$

Notice that the upper bound that $\frac{XY}{1+X+Y} \le \min(X, Y)$ has been widely used in the literature for relaying networks (e.g., [14], [33]) and it is shown to be accurate enough at medium and high SNRs as will be discussed in the results section.

Further, substituting (60) into (17), the OP of D_n for the case $\widehat{R}_k < \widehat{R}_k^{up}$ is lower bounded by

$$\begin{aligned} P_{out}^n &\le 1 - \Pr\left(\min\left(\frac{X}{d_2}, \frac{Y_n}{d_1}\right) > \varepsilon_n^*\right) \\ &= 1 - \Pr\left(\frac{X}{d_2} > \varepsilon_n^*, \frac{Y_n}{d_1} > \varepsilon_n^*\right) \\ &= F_X(d_2\varepsilon_n^*) + F_{Y_n}(d_1\varepsilon_n^*) \\ &\quad - F_X(d_2\varepsilon_n^*)F_{Y_n}(d_1\varepsilon_n^*). \end{aligned} \quad (61)$$

Substituting (58) and (59) into (61), the high-SNR asymptotic OP at D_n is obtained as

$$P_{out}^n \lessapprox \frac{(m_1/\Omega_1)^{m_1}}{m_1!}\left(\frac{d_2\varepsilon_n^*}{\rho}\right)^{m_1} + \frac{N!(m_2!)^{-n}}{(N-n)!n!}\left(\frac{m_2 d_2\varepsilon_n^*}{\Omega_2\rho}\right)^{m_2\cdot n}. \quad (62)$$

Besides, we have $P_{out}^n = 1$ for $\widehat{R}_k \ge \widehat{R}_k^{up}$, irrespective of ρ. This completes of the proof of (19) in Corollary 1.

APPENDIX C
PROOF OF LEMMA 1

After integrating by parts, we can rewrite (25) as

$$\mathbb{E}[Z_n^\mu] = \mu \int_0^{\infty} z^{\mu-1}(1 - F_{Z_n}(z))\mathrm{d}z. \quad (63)$$

Replacing ε_n^* in (18) with z, we can obtain the CDF of Z_n, i.e., $F_{Z_n}(z)$. Substituting the expression of $F_{Z_n}(z)$ into (63) and after some arrangements, we get

$$\mathbb{E}[Z_n^\mu] = \frac{\mu Q_n}{\Gamma(m_2)} \sum_{i_1=0}^{m_1-1} \sum_{j_1=0}^{i_1} \sum_{i_2=0}^{N-n} \sum_{j_2=0}^{n+i_2-1} \sum_{j_2,n_\ell}^{\sim} \sum_{k_2=0}^{m_2+\Phi_{n_\ell}-1} \times \binom{i_1}{j_1} \frac{(\beta_1)^{i_1}}{i_1!} \Lambda(i_2, j_2, n_\ell, k_2) \times \left(\frac{\beta_2}{j_2+1}\right)^{m_2+\Phi_{n_\ell}} \left(\frac{\beta_1 d_1}{\beta_2 d_2}\right)^{\frac{k_2-j_1+1}{2}} \Psi(z), \quad (64)$$

where

$$\Psi(z) = \int_0^{\infty} e^{-(\beta_1+\beta_2)z} z^{i_1+m_2+\Phi_{n_\ell}+\mu-1-\frac{k_2+j_1+1}{2}} \times (z+c)^{\frac{k_2+j_1+1}{2}} K_{k_2-j_1+1}\left(\sqrt{4\beta_1\beta_2 z\,(z+c)}\right) \mathrm{d}z, \quad (65)$$

with $c = \frac{1}{d_1 d_2}$, $\beta_1 = \frac{m_1 d_2}{\Omega_1\rho}$, and $\beta_2 = \frac{(j_2+1)m_2 d_1}{\Omega_2\rho}$.

To facilitate the using of [36, vol.2, eq. (2.16.10.2)], we rewrite (65) as

$$\Psi(z) = \int_0^\infty e^{-(\beta_1+\beta_2)z} z^{i_1+m_2+\Phi_{n_\ell}+\mu-j_1-k_2-2} \times (z+c)^{k_2+j_1+2} \frac{z^{\frac{k_2+j_1+3}{2}-1}}{(z+c)^{\frac{k_2+j_1+3}{2}}} \times K_{k_2-j_1+1}\left(\sqrt{4\beta_1\beta_2 z\,(z+c)}\right) \mathrm{d}z. \quad (66)$$

By using the binomial expansion for $(z+c)^{k_2+j_1+2}$ within the integral, we get

$$\Psi(z) = \sum_{q=0}^{k_2+j_1+2} \binom{k_2+j_1+2}{q} c^q \int_0^\infty z^{i_1+m_2+\Phi_{n_\ell}+\mu-q} \times \frac{e^{-(\beta_1+\beta_2)z} z^{\frac{k_2+j_1+3}{2}-1}}{(z+c)^{\frac{k_2+j_1+3}{2}}} K_{k_2-j_1+1} \times \left(\sqrt{4\beta_1\beta_2 z\,(z+c)}\right) \mathrm{d}z. \quad (67)$$

Consider the following property of the Laplace transform that $\$[t^n f(t)] = (-1)^n \frac{\partial^n F(s)}{\partial s^n}$ [35], where $F(s)$ is the Laplace transform of $f(t)$, i.e., $\$[f(t)] = F(s) \triangleq \int_0^\infty e^{-st} f(t) dt$. With the help of this property, (67) can be rewritten as

$$\Psi(z) = \sum_{q=0}^{k_2+j_1+2} \binom{k_2+j_1+2}{q} c^q (-1)^{i_1+m_2+\Phi_{n_\ell}+\mu-q} \times \frac{\partial^{i_1+m_2+\Phi_{n_\ell}+\mu-q}}{\partial s^{i_1+m_2+\Phi_{n_\ell}+\mu-q}} \Upsilon(s)\Big|_{s=\beta_1+\beta_2}. \quad (68)$$

where

$$\Upsilon(s) = \int_0^\infty e^{-sz} z^{\frac{k_2+j_1+3}{2}-1} (z+c)^{-\frac{k_2+j_1+3}{2}} \times K_{k_2-j_1+1}\left(\sqrt{4\beta_1\beta_2 z\,(z+c)}\right) \mathrm{d}z. \quad (69)$$

Then, with the help of [36, vol.2, eq. (2.16.10.2)], $\Upsilon(s)$ in (69) can be solved as in (27). Finally, by substituting (68) with $\Upsilon(s)$ given in (69) into (64), $\mathbb{E}[Z_n^\mu]$ can be solved as in (26).

APPENDIX D
PROOF OF COROLLARY 2

By assuming $\rho \to \infty$, we get (36) from (33) straightforwardly. Similarly, (37) can be obtained via (34) and (35) as $\rho \to \infty$. Accordingly, the asymptotic ESR of system suffering from RHI can be asymptotically approximated as

$$\begin{aligned} R_{ave}^{sum} &\approx \frac{1}{2}\sum_{n=1}^{N-1} \log_2\left(1+\frac{\alpha_n}{\sum_{j=n+1}^N \alpha_j + d_0}\right) + \frac{1}{2}\log_2\left(1+\frac{\alpha_N}{d_0}\right) \\ &= \frac{1}{2}\log_2\left(\frac{\sum_{j=1}^N \alpha_j + d_0}{\sum_{j=2}^N \alpha_j + d_0} \times \frac{\sum_{j=2}^N \alpha_j + d_0}{\sum_{j=3}^N \alpha_j + d_0} \cdots \times \frac{\alpha_{N-1}+\alpha_N+d_0}{\alpha_N+d_0} \times \frac{\alpha_N+d_0}{d_0}\right) \\ &= \frac{1}{2}\log_2\left(\frac{\sum_{j=1}^N \alpha_j + d_0}{d_0}\right). \end{aligned} \quad (70)$$

Recall that $\sum_{j=1}^N \alpha_j = 1$. Thus we can obtain (38) from (70).

As for the ideal-hardware system, we have

$$\begin{aligned} R_{ave,id}^{sum} &\approx \frac{1}{2}\sum_{n=1}^{N-1} \log_2\left(1+\frac{\alpha_n}{\sum_{j=n+1}^N \alpha_j}\right) + \frac{1}{2}\log_2\left(1+\frac{\alpha_N \Omega_1 \Omega_{2N}}{\Omega_1+\Omega_{2N}}\rho\right) \\ &\overset{(a)}{=} \frac{1}{2}\log_2\frac{1}{\alpha_N} + \frac{1}{2}\log_2\left(1+\frac{\alpha_N \Omega_1 \Omega_{2N}}{\Omega_1+\Omega_{2N}}\rho\right) \\ &= \frac{1}{2}\log_2\left(\frac{1}{\alpha_N} + \frac{\Omega_1\Omega_{2N}}{\Omega_1+\Omega_{2N}}\rho\right), \end{aligned} \quad (71)$$

where (a) is obtained by using the fact $\sum_{n=1}^{N-1} \log_2\left(1+\frac{\alpha_n}{\sum_{j=n+1}^N \alpha_j}\right) = \log_2 \frac{1}{\alpha_N}$. As $\rho \to \infty$, we can obtain (39) from (71).

REFERENCES

[1] Y. Saito, Y. Kishiyama, A. Benjebbour, T. Nakamura, A. Li, and K. Higuchi, "Non-orthogonal multiple access (NOMA) for cellular future radio access," in *Proc. 77th IEEE VTC-Spring*, Dresden, Germany, Jun. 2013, pp. 1–5.
[2] S. M. R. Islam, N. Avazov, O. A. Dobre, and K.-S. Kwak, "Power-domain non-orthogonal multiple access (NOMA) in 5G systems: Potentials and challenges," *IEEE Commun. Surveys Tuts.*, vol. 19, no. 2, pp. 721–742, 2nd Quart., 2016.
[3] Z. Ding, Z. Yang, P. Fan, and H. V. Poor, "On the performance of non-orthogonal multiple access in 5G systems with randomly deployed users," *IEEE Signal Process. Lett.*, vol. 21, no. 12, pp. 1501–1505, Dec. 2014.
[4] S. Timotheou and I. Krikidis, "Fairness for non-orthogonal multiple access in 5G systems," *IEEE Signal Process. Lett.*, vol. 22, no. 10, pp. 1647–1651, Oct. 2015.
[5] Y. Liu, Z. Ding, M. Elkashlan, and J. Yuan, "Nonorthogonal multiple access in large-scale underlay cognitive radio networks," *IEEE Trans. Veh. Technol.*, vol. 65, no. 12, pp. 10152–10157, Dec. 2016.
[6] Z. Ding, M. Peng, and H. V. Poor, "Cooperative non-orthogonal multiple access in 5G systems," *IEEE Commun. Lett.*, vol. 19, no. 8, pp. 1462–1465, Aug. 2015.
[7] N. T. Do, D. B. da Costa, T. Q. Duong, and B. An, "A BNBF user selection scheme for NOMA-based cooperative relaying systems with SWIPT," *IEEE Commun. Lett.*, vol. 21, no. 3, pp. 664–667, Mar. 2017.
[8] L. Lv, Q. Ni, Z. Ding, and J. Chen, "Application of non-orthogonal multiple access in cooperative spectrum-sharing networks over Nakagami-*m* fading channels," *IEEE Trans. Veh. Technol.*, vol. 66, no. 6, pp. 5506–5511, Jun. 2017.
[9] L. Lv, J. Chen, and Q. Ni, "Cooperative non-orthogonal multiple access in cognitive radio," *IEEE Commun. Lett.*, vol. 20, no. 10, pp. 2059–2062, Oct. 2016.
[10] J.-B. Kim and I.-H. Lee, "Capacity analysis of cooperative relaying systems using non-orthogonal multiple access," *IEEE Commun. Lett.*, vol. 19, no. 11, pp. 1949–1952, Nov. 2015.
[11] M. Xu, F. Ji, M. Wen, and W. Duan, "Novel receiver design for the cooperative relaying system with non-orthogonal multiple access," *IEEE Commun. Lett.*, vol. 20, no. 8, pp. 1679–1682, Aug. 2016.
[12] J.-B. Kim and I.-H. Lee, "Non-orthogonal multiple access in coordinated direct and relay transmission," *IEEE Commun. Lett.*, vol. 19, no. 11, pp. 2037–2040, Nov. 2015.
[13] C. Zhong and Z. Zhang, "Non-orthogonal multiple access with cooperative full-duplex relaying," *IEEE Commun. Lett.*, vol. 20, no. 12, pp. 2478–2481, Dec. 2016.
[14] J. Men, J. Ge, and C. Zhang, "Performance analysis of nonorthogonal multiple access for relaying networks over Nakagami-*m* fading channels," *IEEE Trans. Veh. Technol.*, vol. 66, no. 2, pp. 1200–1208, Feb. 2017.

[15] X. Yue, Y. Liu, S. Kang, and A. Nallanathan, "Performance analysis of NOMA with fixed gain relaying over Nakagami-*m* fading channels," *IEEE Access*, vol. 5, pp. 5445–5454, 2017.
[16] Z. Yang, Z. Ding, P. Fan, and N. Al-Dhahir, "The impact of power allocation on cooperative non-orthogonal multiple access networks with SWIPT," *IEEE Trans. Wireless Commun.*, vol. 16, no. 7, pp. 4332–4343, Jul. 2017.
[17] T. Schenk, *RF Imperfections in High-Rate Wireless Systems: Impact and Digital Compensation*. Dordrecht, The Netherlands: Springer, 2008.
[18] E. Costa and S. Pupolin, "M-QAM-OFDM system performance in the presence of a nonlinear amplifier and phase noise," *IEEE Trans. Commun.*, vol. 50, no. 3, pp. 462–472, Mar. 2002.
[19] J. Li, M. Matthaiou, and T. Svensson, "I/Q imbalance in two-way AF relaying," *IEEE Trans. Wireless Commun.*, vol. 62, no. 7, pp. 2271–2285, Jul. 2014.
[20] M. Mokhtar, A.-A. A. Boulogeorgos, G. K. Karagiannidis, and N. Al-Dhahir, "OFDM opportunistic relaying under joint transmit/receive I/Q imbalance," *IEEE Trans. Commun*, vol. 62, no. 5, pp. 1458–1468, Jul. 2014.
[21] N. Maletic, M. Cabarkapa, N. Neskovic, and D. Budimir, "Hardware impairments impact on fixed-gain AF relaying performance in Nakagami-*m* fading," *Electron. Lett.*, vol. 52, no. 12, pp. 121–122, Jul. 2016.
[22] E. Balti and M. Guizani, "Impact of non-linear high-power amplifiers on cooperative relaying systems," *IEEE Trans. Commun.*, vol. 65, no. 5, pp. 4163–4175, Jul. 2017.
[23] X. Zhang, M. Matthaiou, M. Coldrey, and E. Björnson, "Impact of residual transmit RF impairments on training-based MIMO systems," *IEEE Trans. Commun.*, vol. 63, no. 8, pp. 2899–2911, Aug. 2015.
[24] N. I. Miridakis and T. A. Tsiftsis, "On the joint impact of hardware impairments and imperfect CSI on successive decoding," *IEEE Trans. Veh. Technol.*, vol. 66, no. 6, pp. 4810–4822, Jun. 2017.
[25] E. Bjornson, M. Matthaiou, and M. Debbah, "A new look at dual-hop relaying: Performance limits with hardware impairments," *IEEE Trans. Commun.*, vol. 61, no. 11, pp. 4512–4525, Nov. 2013.
[26] M. Matthaiou, A. Papadogiannis, E. Björnson, and M. Debbah, "Two-way relaying under the presence of relay transceiver hardware impairments," *IEEE Commun. Lett.*, vol. 17, no. 6, pp. 1136–1139, Jun. 2013.
[27] P. K. Sharma and P. K. Upadhyay, "Cognitive relaying with transceiver hardware impairments under interference constraints," *IEEE Commun. Lett.*, vol. 20, no. 4, pp. 820–823, Apr. 2016.
[28] T. T. Duy, T. Q. Duong, D. B. D. Costa, V. N. Q. Bao, and M. Elkashlan, "Proactive relay selection with joint impact of hardware impairment and co-channel interference," *IEEE Trans. Commun.*, vol. 63, no. 5, pp. 1594–1606, May 2015.
[29] A. K. Mishra, D. Mallick, and P. Singh, "Combined effect of RF impairment and CEE on the performance of dual-hop fixed-gain AF relaying," *IEEE Commun. Lett.*, vol. 20, no. 9, pp. 1725–1728, Sep. 2016.
[30] K. Guo, B. Zhang, Y. Huang, and D. Guo, "Outage analysis of multi-relay networks with hardware impairments using SECps scheduling scheme in Shadowed-Rician channel," *IEEE Access*, vol. 5, pp. 5113–5120, Mar. 2017.
[31] D. B. da Costa and S. Aïssa, "Capacity analysis of cooperative systems with relay selection in Nakagami-*m* fading," *IEEE Commun. Lett.*, vol. 13, no. 9, pp. 637–639, Sep. 2009.
[32] H. Holma and A. Toskala, *LTE for UMTS: Evolution to LTE-Advanced*, 2nd ed. Hoboken, NJ, USA: Wiley, 2011.
[33] S. Ikki and M. H. Ahmed, "Performance analysis of cooperative diversity wireless networks over Nakagami-*m* fading channel," *IEEE Commun. Lett.*, vol. 11, no. 4, pp. 334–336, Apr. 2007.
[34] D. Senaratne and C. Tellambura, "Unified exact performance analysis of two-hop amplify-and-forward relaying in Nakagami fading," *IEEE Trans. Veh. Technol.*, vol. 59, no. 3, pp. 1529–1534, Mar. 2010.
[35] I. S. Gradshteyn and I. M. Ryzhik, *Table of Integrals, Series and Products*, 7th ed. San Diego, CA, USA: Academic, 2007.
[36] A. P. Prudnikov, Y. A. Brychov, and O. I. Marichev, *Integrals and Series*, vols. 1–5. Amsterdam, The Netherlands: Gordon Breach Science Publishers, 1986.

FAN DING received the B.S. degree in electronic information science and technology from the School of Electronic Information, and the M.S. degrees in electronic circuit and system from the Global Navigation Satellite System Center, Wuhan University, China, in 2006 and 2009, respectively, and the Ph.D. degree from the Department of Information Engineering, Shenzhen University, in 2017. In 2010, he joined the School of Physics and Electromechanical Engineering, Shaoguan University, China, where he is currently a Lecturer. His research interests include cooperative communication, cognitive radio, physical layer security, and non-orthogonal multiple access technologies.

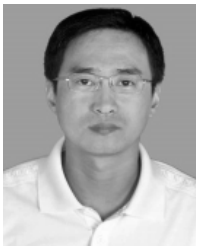

HUI WANG received the B.S., M.S., and Ph.D. degrees from Xian Jiaotong University in 1990, 1993, and 1996, respectively. He is currently a Professor with the College of Information Engineering, Shenzhen University. His research interests include wireless communication, signal processing, and distributed computing systems, in which he is the author or co-author of more than 50 international leading journals, conferences, and book chapters.

SHENGLI ZHANG received the B.Eng. degree in electronic engineering and the M.Eng. degree in communication and information engineering from the University of Science and Technology of China (USTC), Hefei, China, in 2002 and 2005, respectively, and the Ph.D. degree from the Department of Information Engineering, The Chinese University University of HongKong (CUHK), in 2008. From 2002 to 2005, he was with the Personal Communication Network and Spread Spectrum Laboratory, USTC, as a Research Engineer involved in several National 863 Research Projects including the Beyond-3 Generation of Mobile System in China (FUTURE Plan). From 2002 to 2005, he was a Research Engineer with the UTStarcom Wireless Soft Research Center, Hefei, China, involved in the research and implementation of WCDMA communication systems. In 2008, he was a Research Associate at CUHK. He is currently a Professor with the Communication Engineering Department, Shenzhen University, China. His current research interests include wireless networks, wireless communication, physical layer network coding, and cooperative wireless networks.

MINGJUN DAI received the Ph.D. degree in electronic engineering from the City University of Hong Kong in 2012. He is currently an Associate Professor with the College of Information Engineering, Shenzhen University, China. His research interests include cooperative relay network, network coding design, and optimization of wireless networks.